

Candidates for three-quasiparticle K -isomers in even-odd Fm - Cn nuclei

P. Jachimowicz¹, M. Kowal^{2,*} and J. Skalski²

¹ *Institute of Physics, University of Zielona Góra,
Z. Szafrana 4a, 65-516 Zielona Góra, Poland and*

² *National Centre for Nuclear Research,
Pasteura 7, 02-093 Warsaw, Poland*

(Dated: August 19, 2025)

Abstract

Following our study of possible K -isomers in odd-even Md-Rg nuclei, here we continue with searching for three-quasiparticle $1\nu 2\pi$ and 3ν isomer candidates in even-odd Fm - Cn nuclei. We use the same approach to calculate energies of different nuclear configurations using a microscopic-macroscopic model with the Woods-Saxon potential. We used two versions of pairing: quasi-particle BCS method and particle number projection formalism. The optimal deformations for both ground states and high- K configurations are determined through a four-dimensional energy minimization process. We point out the most promising candidates for high- K isomers and compare them, where possible, with existing experimental data.

*Electronic address: michal.kowal@ncbj.gov.pl

I. INTRODUCTION

Recent progress in experimental techniques will soon make it possible to conduct more systematic studies of excited states in superheavy (SH) nuclei, and enable them in systems with $Z > 105$. Among various excitations, isomeric high- K states present a special interest, providing some information on low-lying single-particle (s.p.) orbitals and mechanisms of decay hindrance. The already established presence of high- K isomers and characteristics of the rotational bands in the No–Rf region [48, 49, 51] are consistent with results of realistic microscopic-macroscopic (MM) and mean-field models, which predict well-deformed axially symmetric shapes and numerous high- Ω orbitals close to the Fermi levels in these nuclei. In the present work, following the previous one [61] devoted to three-quasiparticle (3qp) high- K isomers in odd-even nuclei, we present predictions for 3qp isomers in even-odd Fm–Cn nuclei using the micro-macro (MM) model with the Woods-Saxon potential, extensively studied in the region of heavy and SH nuclei.

Since all nuclear models of superheavy nuclei (SHN) are merely extrapolations from better-known regions of the nuclear chart, and experimental data on the structure of $Z \geq 100$ systems is still scarce, an appreciation as to the correctness of the former or the agreement or disagreement of both is rather fragmentary at present. It is even more so, as often the only certain experimental result is the isomer half-life with some bounds on its spin and energy. Then the spin value and configuration assignments are given partially based on some theoretical result.

While it can be said that predictions of (the candidates for) isomeric high- K states reflect mostly the structure of the s.p. spectra, one has to remember that these spectra depend on equilibrium deformations, and those change, even if a little, from isotope to isotope. In this situation, only the more prominent features of the predicted high- K configurations qualify for the model vs experiment test.

In the context of many-q.p. excitations, the important feature of the present model is the distinct subshell gap in the neutron spectrum at $N = 152$ around fermium and nobelium, which seem necessary for realistic predictions of K -isomeric states. Two other subshell gaps predicted by the model: at $N = 162$ for neutrons and at $Z = 108$ for protons, not quite confirmed experimentally yet, strongly influence the predictions presented here. The very similar Woods-Saxon model was used in [62, 63], which can be consulted for predictions

concerning 1-q.p. proton and neutron excitations in this region of nuclei.

Up to now, high- K isomers have been identified in a few even-odd nuclei. Low-energy, one-quasiparticle states were found in ^{253}Fm (at ≈ 350 keV) [16], ^{255}No (at 240–300 keV [17] or 225 keV [18]) and ^{257}Rf (at ≈ 75 keV) [23], interpreted as the $\nu 11/2^-$ [725] structure. 3qp isomers were found in $^{251,253,255}\text{No}$ (one [13, 19], one [14–16] and two [17, 18], respectively) and in $^{253,255,257}\text{Rf}$ (one [19, 20], two [21, 22] and one [23–25], respectively), and one supposedly 5qp isomer in ^{255}No [18]. Spins and energies of two 3qp isomers in ^{255}No were reported in [18], spins and energies for ^{255}Rf were given in [21, 22] and energy of the 3qp isomer in ^{257}Rf in [25]. Properties of known isomers in neighbouring even-even Fm, No, and Rf nuclei have an impact on the proposed assignments of the quasiparticle structure. An example is provided by the 0.28 s, 8^- isomer in ^{254}No [8, 11, 12], the structure of which is related to that of isomers in $^{251,253}\text{No}$ and $^{254,255}\text{Rf}$ [90]. At the moment, the question of whether it is a two-proton or two-neutron structure is unsettled [41]. The recent collection of data on isomers in the heaviest nuclei is given in [26, 27], see also Ackermann et al. [86], Asai et al. [39], Dracoulis et al. [44], Walker et al. [45], and A. Lopez-Martens with K. Hauschild [41].

We search for K -isomers by calculating equilibrium energies of many high- K 3qp configurations, both $1\nu 2\pi$ and 3ν , formed from low-lying quasiparticle states. The set of studied 3qp states contains traditionally considered high- K configurations called “optimal” (i.e., obtained by the tilted Fermi surface method), but is considerably larger. For a theoretical overview based on the Nilsson-Strutinsky approach, see the work by Walker et al. (2016) [6]. As in the study on odd-even nuclei, we consider variants of pairing treatment: the quasiparticle method, and particle number projection that avoids deficiencies of the former, particularly for 3-neutron q.p. excitations. In the present work, we studied nuclei in the following range of neutron numbers: $N = 141$ –167 for Fm, No, Rf, Sg; $N = 143$ –169 for Hs; $N = 145$ –171 for Ds; and $N = 147$ –173 for Cn.

The calculations and selection of candidates for high- K isomers are described in Sect. II, and results are presented and discussed in Sect. III. The conclusions are given in Sect. IV.

II. THE METHOD

We use the MM method with the deformed Woods-Saxon (WS) potential [52] and the macroscopic Yukawa-plus-exponential energy model [53] with parameters specified in [54].

Parameters of the model are kept the same as in all recent applications to heavy and superheavy nuclei, which concern masses and deformations [55], Q_α - energies [56], the first and second fission barriers in actinides [57] and SH nuclei [58], [59]. In order to obtain ground-states and configuration-constrained minima, we use a four-dimensional space of deformations $\beta_{\lambda 0}$ defining the nuclear surface:

$$R(\theta) = c(\beta)R_0 \left[1 + \sum_{\lambda=2,4,6,8} \beta_{\lambda 0} Y_{\lambda 0}(\theta) \right], \quad (1)$$

where $Y_{\lambda 0}(\theta)$ are spherical harmonics, $c(\beta)$ is the volume-fixing factor depending on deformation, and R_0 is the radius of a spherical nucleus. Deformation parameters beyond β_{20} and β_{40} turned out necessary in studies of g.s. and high-K configuration equilibria in very heavy nuclei [64, 65],[66]. On the other hand, calculations within our MM model [59] showed that the reflection-asymmetric axial equilibrium deformations of the considered nuclei are either zero or negligible, so their omission is substantiated. Therefore, the intrinsic parity of the considered states is well-defined.

Four-dimensional energy minimization over $\beta_{20}, \beta_{40}, \beta_{60}, \beta_{80}$ (1) was performed using the gradient method. To avoid secondary or very deformed minima, the minimization is repeated at least 10 times for each configuration with different starting values of deformations.

In the previous work, dealing with candidates for 3qp isomers in heavy odd-even nuclei, we have found that blocking two, and especially three quasi-particles in the BCS procedure (blocking approximation) produce a too small or vanishing pairing gap and too low 3qp excitation energies. Therefore, in the present study, we use exclusively the quasi-particle method and the particle-number-projection method (PNP).

In the quasiparticle method, the microscopic part of the energy for a $1\nu 2\pi$ configuration is taken as the sum of BCS quasi-particle energies of singly occupied levels:

$$E_{q.p.}^* = \sqrt{(\epsilon_\nu - \lambda_\nu)^2 + \Delta_\nu^2} + \sqrt{(\epsilon_{\pi_1} - \lambda_\pi)^2 + \Delta_\pi^2} + \sqrt{(\epsilon_{\pi_2} - \lambda_\pi)^2 + \Delta_\pi^2} \quad (2)$$

and the core energy term consisting of the shell and pairing corrections calculated without blocking. The total, i.e., including the macroscopic part, energy, is then minimized over deformations. For neutrons, the core term, as well as the pairing gap Δ_ν and the Fermi energy λ_ν , are calculated for the odd number of particles, but with the double occupation of

all levels. This prescription was used before in [63]. For 3ν q.p. excitations, the microscopic energy was the sum of three neutron-quasiparticle energies and the shell and pairing corrections calculated without blocking. As for the $1\nu 2\pi$ excitations, the odd particle number and double occupation of levels were used in the BCS procedure for neutrons. In the quasiparticle method, we use the same pairing strengths as in our mass model ($I = (N - Z)/A$): $G_p = (g_{0p} + g_{1p}I)/A$ for protons and $G_n = (g_{0n} + g_{1n}I)/A$ for neutrons, with $g_{0p} = 13.40$ MeV, $g_{1p} = 44.89$ MeV, $g_{0n} = 17.67$ MeV, $g_{1n} = -13.11$ MeV.

One should mention that the quasiparticle method, especially for 3ν -q.p. excitations, has several flaws. First, it underestimates excitation energies at particle numbers for which the BCS energy gap vanishes or is minimal. This happens in the vicinity of substantial gaps in the s.p. spectrum, for odd $N = N_{gap} \pm 1$, with N_{gap} the number of neutrons on levels below the gap. Moreover, if two additional levels are blocked above the gap for $N = N_{gap} + 1$, or below the gap for $N = N_{gap} - 1$, their excitation energies are underestimated further. In the former case, the Fermi energy of the core (accounting for half of the BCS occupancy of the level above the gap) lies just below the upper edge of the gap. Blocking two additional levels above the gap requires that the Fermi level of the $N_{gap} - 2$ *paired* particles be lowered to ensure the correct (expectation value of the) particle number. In the latter case, the Fermi level of the core lies just above the lower edge of the gap while the Fermi energy of the $N_{gap} - 4$ paired particles should be elevated as two of them must be promoted above the gap. The related increase in energy of the 3qp states is not reflected in the sum of quasi-particle energies (2) as the Fermi energy of the core is close to the s.p. energies of two additional blocked levels.

In order to correct for the related error, one could adjust the Fermi level of the core for each set of blocked levels to obtain the correct number of paired particles $\langle \hat{N}_{pair} \rangle = N - 3$ on unblocked levels while keeping Δ_ν of the core unchanged (ignoring the second BCS equation). We have checked that this gives a correction in the right direction. On the other hand, such a procedure does not seem worthwhile in comparison to the PNP solution, so we did not pursue it further. We have also made a second 3ν q.p. calculation with the core taken as the system of $N - 1$ (even number of) particles. While both sets of results have some places in which the abovementioned errors occur, the second one produces more physical results for isotones $N = N_{gap} + 1$.

We use the Particle Number Projection (PNP) in order to correct for known deficiencies

of the Bardeen-Cooper-Schrieffer (BCS) method in the weak pairing regime. The procedure is to select the component of the BCS-like state $\Psi(\lambda, \Delta)$ (with Δ and λ unrestricted by the BCS equations) with exactly n pairs of particles, and calculate on it the expectation value E_n of the pairing Hamiltonian. This should be done independently for the neutron and proton subsystems ($2n = Z$ or $Z - 2$ for g.s. or 2π q.p. states, and $N - 1$ or $N - 3$ for 1ν or 3ν q.p. states).

In the majority of calculations, we used the well-known method of Fomenko [60]. We also implemented a second method for the purpose of tests, which consists in expressing E_n in terms of norms of particle-projected BCS-like states:

$$E_n = \frac{\sum_{\mu>0} (2\epsilon_\mu - G) v_\mu^2 P_{n-1}^\mu - G \sum_{\mu>0 \neq \nu>0} u_\mu v_\mu u_\nu v_\nu P_{n-1}^{\mu\nu}}{P_n}, \quad (3)$$

where P_n , P_{n-1}^μ and $P_{n-1}^{\mu\nu}$ are the squared norms of: the n -pairs component of $\Psi(\lambda, \Delta)$, the $n - 1$ pairs component of $\Psi(\lambda, \Delta)$ with the level μ excluded, and the $n - 1$ pairs component of $\Psi(\lambda, \Delta)$ with excluded levels μ and ν , respectively; ϵ_μ are s.p. energies, G - the pairing strength, u_μ and v_μ - BCS-like amplitudes. Since P_n is the coefficient by ζ^n of the polynomial $\prod_{\nu>0} (u_\nu^2 + \zeta v_\nu^2)$, one can find it by representing ζ as the $(n + 1)$ -dimensional Jordan block with zeros on the main diagonal and one on the first superdiagonal and calculating the element $(n + 1, n + 1)$ of the matrix product $\prod_{\nu>0} (u_\nu^2 \mathbb{I} + \zeta v_\nu^2)$. Quantities P_{n-1}^μ can be obtained in the same way, and from them $P_{n-1}^{\mu\nu}$ - see Appendix of [61]. Both computational schemes were checked to give identical results for E_n .

To simplify the search for the optimal projected BCS-like state into a single-parameter minimization, parameter λ of $\Psi(\lambda, \Delta)$ is fixed by requiring that the expectation value of the particle number operator, $\langle \Psi(\lambda, \Delta) | \hat{N} | \Psi(\lambda, \Delta) \rangle$, be equal the desired number of particles. The resulting projected energy is then a function of Δ alone and exhibits a unique minimum. This minimal value is adopted as the energy after projection. For each configuration, the minimization of E_n over Δ is performed at each step of the minimization over deformation.

In the previous work [61], we have chosen pairing strengths $G_n(N, Z)$ for neutrons and $G_p(N, Z)$ for protons in the PNP procedure as: $G_n(N, Z) = 1.1 G_n^{mod}(N, Z)$, $G_p(N, Z) = 1.1 G_p^{mod}(N, Z)$, with $G_n^{mod}(N, Z)$, $G_p^{mod}(N, Z)$ the pairing strengths from our MM model. With this choice, we obtained the energy of the 2-q.p. neutron excitations involving two nearly degenerate s.p. levels at the Fermi energy: the last occupied and the first empty one, close to $2\Delta_n(\text{BCS})$ of our MM model, while the proton strengths ratio G_p/G_p^{mod} was chosen

equal to that for neutrons. In the present calculations, we first used the same parameters. After noticing that the smallest excitation energies of 3ν q.p. states of ≈ 0.65 MeV are clearly too small, we made a second calculation with $G_n(N, Z) = 1.15 G_n^{mod}(N, Z)$. The pairing strength for protons was kept the same, as it has a negligible effect on 3ν q.p. state energies. As a result, the smallest energy of the 3ν q.p. states increased to ≈ 1 MeV, which looks more realistic. One can notice that the neutron pairing strength G_n practically does not influence energies of the $1\nu 2\pi$ q.p. states.

Equilibrium deformations were found by the quasiparticle method for 6012 $1\nu 2\pi$ configurations with $K_\pi = \Omega_{\pi 1} + \Omega_{\pi 2} \geq 5$ and 5824 3ν q.p. configurations with $K_\nu = \Omega_{\nu 1} + \Omega_{\nu 2} + \Omega_{\nu 3} \geq 11/2$ built from s.p. states not too distant from the Fermi surfaces in the studied nuclei. Using these results as a guidance, the PNP calculations were confined to some selected low-lying 3qp states. Configurations at the lowest excitation energies $E_{3q.p.}^*(K)$ are considered as likely candidates for K -isomers. The angular momentum I of the 3q.p. configuration is understood as a sum of s.p. angular momentum projections Ω_i . We did not consider shifts due to the spin interaction (counterpart of Gallagher shifts for 2q.p.), which for 3q.p. configurations are not well understood [77, 78].

As mentioned in our study of odd-even systems [61], an additional indicator of possible isomerism of the high- K 3-q.p. configuration may be its excitation above the state of the same spin of the collective rotational band built on its 1ν q.p. component (more loosely, its excitation above the yrast line). The rotational energy of the 1ν collective band with $K_\nu = \Omega_\nu$ and the band-head at the excitation energy $E_{1q.p.}^*(\Omega_\nu)$ (which would be zero for the g.s.) can be estimated as: $E^{rot}(I = K, \Omega_\nu) = \frac{1}{2}[K(K+1) - \Omega_\nu^2]/\mathcal{J}$, with \mathcal{J} - average moment of inertia of the 1-neutron q.p. rotational band. The smaller the value $[E_{3q.p.}^*(K) - E_{1q.p.}^*(\Omega_\nu) - E^{rot}(I = K, \Omega_\nu)]$, the less probable is the high- K 3 q.p. state deexcitation to the one-neutron q.p. rotational band. Thus, for $1\nu 2\pi$ states, a large extra-aligned $K_{2\pi} = K_{\pi 1} + K_{\pi 2}$ of the two-proton pair is favourable for the isomer existence. For a 3ν configuration, decays are possible to three rotational bands built on each 1ν component. The most probable of them would limit the isomer existence. In particular, if $K_{\nu 1}$ and $K_{\nu 2}$ are much smaller than $K_{\nu 3}$, and three excitation energies of 1ν band-heads are similar, the stringest condition for 3ν isomer would be a decay to the rotational band built on $K_{\nu 3}$ - its rotational energy E^{rot} is the smallest as it corresponds to the smallest collective angular momentum $K_{\nu 1} + K_{\nu 2}$ (equal or similar moments of inertia are tacitly assumed for all 1ν rotational bands).

As in [61] we used the calculated cranking moments of inertia of even-even nuclei from [68] to estimate rotational energies in studied isotopes. For odd- N nuclei, we took the average from the calculated moments of inertia in neighboring even-even nuclei and increased it by a factor 1.4.

III. RESULTS AND DISCUSSION

At present, experimental information on even-odd Fm-Cn nuclei exists for neutron numbers between $N = 141$ -159 for Fm, $N = 147$ -157 for No, $N = 149$ -163 for Rf, $N = 153$ -163 for Sg, $N = 155$ -169 for Hs, $N = 157$ -171 for Ds and $N = 165$ -173 for Cn.

Equilibrium deformations obtained for studied nuclei in our MM model with the q.p. method are shown in Fig. 1 (very similar deformations obtained with the blocking method are reported in [59]). Deformation β_{20} in Fm-Hs is mostly in the range 0.23-0.25, with a wide maximum around $N = 153$ -157, slightly decreasing towards 0.19 - 0.20 for larger N ; in Ds and Cn it is smaller, with a sharp decrease for $N = 171$. Deformations β_{40} mostly decrease with N from a wide maximum at $N = 143$ towards a value by ≈ 0.1 smaller at $N = 167$; they show a spread in Z , with larger values occurring mostly for smaller Z . Deformation β_{60} shows a wide minimum around $N \approx 155$. It changes within a range of ≈ 0.06 for each element, and at fixed N it mostly increases with Z . Deformation β_{80} is generally small, showing roughly a sinusoidal pattern as a function of N , with the values $\approx 0.02 - 0.03$ at the maximum around $N = 158, 160$. Equilibrium deformations for the majority of 3q.p. configurations are mostly close to those of the ground states, but the differences in β_{20} can reach sometimes 0.02 - 0.03. In the PNP method, equilibrium deformations are in most cases very similar to those in the q.p. method, with a tendency towards slightly smaller values.

Ground-state spins and parities of the considered odd- N nuclei are usually (but not always) determined by the s.p. spectrum - properties of the singly occupied neutron orbital at the Fermi level. Results obtained in the quasiparticle scheme are shown in Fig. 2. The g.s. spins and parities from the PNP calculation (indicated in Fig. 2 in red only if different from q.p. result) differ from the above only when the neutron Fermi level falls in the vicinity of nearly degenerate neutron orbitals.

Characteristic of the s.p. neutron spectrum in our Woods-Saxon model are two gaps at $N = 152$ and 162. Below the lower gap one has (from $N = 141$ up) the following states:

$1/2_{13}^-$ [501], $7/2_5^-$ [743], $1/2_{13}^+$ [631], $5/2_7^+$ [622], $7/2_4^+$ [624], and $9/2_3^-$ [734]; between the gaps there are five orbitals: $1/2_{14}^+$ [620], $3/2_{10}^+$ [622], $11/2_2^-$ [725], $7/2_5^+$ [613] and $9/2_3^+$ [615]; above the $N=162$ gap there are following states: $13/2_1^-$ [716], $9/2_4^+$ [604], $3/2_{11}^+$ [611] and $5/2_8^+$ [613]. For neutron numbers $N = 169, 171, 173$ in Hs, Ds, and Cn, the equilibrium deformations β_{20} are significantly smaller and the following additional states are close to the Fermi level: $11/2_2^+$ [606], $1/2_{15}^+$ [611], $15/2_1^-$ [707] (Single-particle (s.p.) states are denoted by Ω_n^π), where Ω is the projection of the s.p. total angular momentum onto the symmetry axis, π is its parity, and the subscript ‘n’ is the ordinal number of the state (with a given Ω^π) counted from the lowest energy within that Ω^π block. Additionally, states may be identified by their asymptotic Nilsson quantum numbers $[Nn_z\Lambda]$ (where N is the principal quantum number, n_z the oscillator quanta along the symmetry axis, and Λ the projection of orbital angular momentum). In Fig. 3, the calculated s.p. neutron levels at equilibrium deformations are shown for four nuclei: ^{253}No , ^{261}Sg , ^{275}Ds and ^{283}Cn .

Experimentally established ground state spins and parities are: in odd- N isotopes $^{249-257}\text{Fm}$: $7/2^+$, $9/2^-$, $1/2^+$, $7/2^+$ and $9/2^+$, and in four nobelium isotopes $^{249,253,255,259}\text{No}$: $5/2^+$, $1/2^+$, $9/2^-$ and $9/2^+$ [28]. The g.s. configurations calculated within the PNP method are different in ^{255}Fm and ^{257}Fm , in which the experimental configurations come out excited, respectively, by 140 and 160 keV, and in ^{259}No , in which the experimental configuration is obtained at the excitation of 170 keV. These comparisons suggest a slightly different order or spacing of neutron levels, in particular, a higher placement of the $\nu 11/2_2^-$ state and a lower one of the $\nu 7/2_5^+$ and $9/2_3^+$ states. The left-hand part of Fig. 3 shows the relative positions of the neutron levels above the $N = 152$ gap, relevant for the above comparison.

A. Excitation energies of $1\nu 2\pi$ 3-q.p. high- K candidates for isomeric states

The low-lying $1\nu 2\pi$ high- K configurations involve single-neutron states situated near the neutron Fermi level coupled to low-lying two-proton (2π) excitations characterized by large K values. In Figures 5 through 11 are presented excitation energies $E_{\nu\pi 2}^*$ of such configurations in isotopes of studied elements obtained from the quasiparticle method (the bottom parts) and the PNP calculation (the top parts). As may be seen there, the composition of the favoured 2π excitations changes with increasing proton number Z from Fm to Cn. These changes can be also seen in Fig. 4, where s.p. proton levels are shown for four chosen

nuclei at their calculated equilibrium deformations.

For Fm ($Z = 100$), it is the $\pi^2 7^- \{7/2_3^- \otimes 7/2_3^+\}$ proton pair, leading to excitation energies $\gtrsim 1.5$ MeV. In No ($Z = 102$) and Rf ($Z = 104$), configurations such as $\pi^2 5^- \{9/2_2^+ \otimes 1/2_{10}^+\}$ and $\pi^2 8^- \{7/2_3^- \otimes 9/2_2^+\}$ become energetically favorable, with some states in Rf exhibiting excitation energies around 1.0–1.2 MeV, particularly in the $N \approx 147$ –155 region. In Sg ($Z = 106$), proton pairs like $\pi^2 6^+ \{7/2_3^- \otimes 5/2_5^-\}$ and $\pi^2 7^- \{9/2_2^+ \otimes 5/2_5^-\}$ contribute to low-lying states, with the quasiparticle calculations indicating minima around 1.1 MeV for $N \approx 145$ –155. The influence of the $Z = 108$ proton shell closure becomes apparent in Hs, where configurations involving orbitals above this gap, such as $\pi^2 7^+ \{5/2_5^- \otimes 9/2_2^-\}$ and $\pi^2 8^- \{5/2_5^- \otimes 11/2_1^+\}$, are significant, with calculated excitation energies generally above 1.3 MeV. Finally, for the heaviest elements considered, Ds ($Z = 110$) and Cn ($Z = 112$), key proton pairs are $\pi^2 10^- \{9/2_2^- \otimes 11/2_1^+\}$, $\pi^2 7^- \{3/2_8^- \otimes 11/2_1^+\}$, and $\pi^2 6^+ \{3/2_8^- \otimes 9/2_2^-\}$, with the lowest quasiparticle excitation energies predicted around 1.2–1.3 MeV, particularly for Ds near $N = 163$, while energies in Cn are generally somewhat higher.

Each of the Figures 5-11 presents results for *the same configurations*. While the energies obtained for selected configurations in the quasiparticle method are shown for all even-odd isotopes (within the chosen energy window), the PNP energies were calculated mostly over isotope ranges where they would be among the lowest ones. Hence a more comprehensive view of an isotopic dependence of $E_{\nu\pi^2}^*$ for each configuration can be obtained from the bottom parts of these figures.

One feature visible in Figures 5-11 is an abrupt change in energy of $1\nu 2\pi$ configurations between isotopes $N - 1$ and $N + 1$ for $N = 152$ and 162 . Its origin are the gaps in the s.p. neutron spectrum at $N = 152$ and $N = 162$, as a neutron state just below the gap, close to the Fermi level at $N - 1$, becomes distant from it at $N + 1$, while a level above the gap at $N - 1$ becomes closer to the Fermi level at $N + 1$. Another noticeable feature is the increase in $1\nu-2\pi$ energies with N , very pronounced in Fm, less so in No and Rf, and even weaker for larger Z . This behavior largely reflects the variation of the proton pairing gap Δ : it increases with N in Fm, No, and Rf, but the increase becomes progressively smaller with Z , and disappears entirely for Sg–Cn.

Below, we comment on results for successive isotopic chains.

Fm The majority of the lowest-lying high- K $1\nu 2\pi$ configurations in Fm isotopes contain the $\pi^2 7^- \{7/2_3^+ \otimes 7/2_3^-\}$ pair coupled to the lowest-lying one-neutron states (still lower lying

configurations with the $\pi^2 4^- \{7/2_3^+ \otimes 1/2_{10}^-\}$ pair are omitted as having $K_{2\pi} < 5$). Energies from the PNP formalism, shown in the upper panel of Fig. 5, rise with N from 1.3 to ≈ 2.8 MeV. The lowest energies, around 1.3–1.4 MeV, are predicted for the lightest isotopes ($N = 141$ – 143). A moderate increase in energy is observed up to $N = 149$, followed by a significant rise for heavier isotopes. Configurations with the proton pair $\pi^2 5^- \{7/2_3^+ \otimes 3/2_7^-\}$ (not shown in figure as having smaller $K_{2\pi}$) lie slightly lower in $N = 145, 147, 149$ isotopes, where they are nearly degenerate with those shown in Fig. 5.

The quasiparticle method (lower panel in Fig. 5) yields a qualitatively similar picture for excitation energies, although their rise with N is milder than for the PNP results.

Overall, excitation energies obtained for even-odd Fm nuclei suggest that low-lying $1\nu 2\pi$ high- K isomers could be expected only in lighter isotopes.

No The lowest-lying $1\nu 2\pi$ high- K configurations have two-proton components $\pi^2 5^- \{1/2_{10}^- \otimes 9/2_2^+\}$ (circles and squares in Figure 6) and $\pi^2 8^- \{7/2_3^- \otimes 9/2_2^+\}$ (triangles and diamonds) - Fig. 6.

In the PNP calculations (upper panel) the configurations involving the $\pi^2 \{1/2_{10}^- \otimes 9/2_2^+\}$ pair (circles, squares) lie systematically lower in lighter isotopes, reaching a minimum of about 1.45 MeV for $N = 149, 151$ (green circles) and 153 (black circle). In contrast, the configurations built on the $\pi^2 \{7/2_3^- \otimes 9/2_2^+\}$ pair (triangles, diamonds) are predicted at excitation energies above 1.7 MeV for $N \leq 151$. This comes from the $K_{2\pi} = 8^-$ state being non-optimal which generates an additional energy cost. The energy difference between two sets of configurations decreases towards $N = 159$, where they become nearly degenerate. All energies sharply increase with N for $N > 152$ to ≈ 2.5 MeV at $N = 167$.

In the quasiparticle method (lower panel), the separation between energies of configurations involving $K_{2\pi} = 5$ and 8 two-proton pairs is small, ≤ 100 keV (as in the quasiparticle method a downward shift of the Fermi level is not accounted for). While the lowest energy of ≈ 1.45 MeV is also found at $N = 149 - 153$ (green and black circles), the rise in excitation energies with N for $N > 152$ is less steep.

Energies of excitation above the rotational g.s. structure, discussed in Sect. II, estimated in the quasiparticle method are: in $N = 151$, for the $\nu 9/2_3^-$ g.s. configuration coupled to $K_{2\pi} = 5$ and $K_{2\pi} = 8$ pairs (green circle and triangle) - respectively ≈ 1.1 MeV and ≈ 0.75 MeV; in $N = 153$, for the $\nu 1/2_{14}^+$ g.s. coupled to $K_{2\pi} = 5$ and $K_{2\pi} = 8$ pairs (black circle and triangle) - ≈ 1.3 MeV and ≈ 1.1 MeV. In the PNP method, these excitations are similar

for states involving the $K_{2\pi} = 5$ pair, but 300 - 400 keV larger for those with the $K_{2\pi} = 8$ component. This does not suggest an isomeric character of the state composed of the 8^- proton pair and the $1/2_{14}^+$ neutron in ^{255}No . Slightly smaller excitations are estimated in the quasiparticle method for configurations with the $\nu 11/2_-^-$ state coupled to both proton pairs (yellow square and diamond) in ^{255}No , but they remain large in the PNP method (see the comparison with the experimental data at the end of this section).

In conclusion, both calculation methods point to the $N \approx 149$ region as having the lowest excitation energies, around 1.4–1.5 MeV. Since in the quasiparticle method energies of the higher- K states involving the 8^- proton pair are lower, it gives a more favourable prediction for their isomeric character; within the more reliable PNP method such a conclusion is uncertain.

Rf The same two-proton pairs as in No enter the lowest-lying high- K $1\nu 2\pi$ states in Rf isotopes - see Fig. 7. As the $K_{2\pi} = 8$ pair is now the optimal one (see Fig. 4) the order of two types of configurations is inverted (note the exchange of symbols between Figures 6 and 7), except for $N = 161$ -167. In addition, in the heaviest isotopes, the proton pair $\pi^2 7^- \{9/2_2^+ \otimes 5/2_5^-\}$ appears as forming the second lowest $1\nu 2\pi$ configuration in $N = 167$, and, within the quasiparticle method, in $N = 165$.

It is noteworthy that $1\nu 2\pi$ energies calculated in Rf are clearly lower than in Fm and No. The lowest energies, ≈ 1 MeV in PNP, and ≈ 1.2 MeV in the quasiparticle method, occur in $N = 149, 151, 153$ isotopes. Since configurations containing the higher- $K_{2\pi}$ proton pair are now lower in energy, their excitation above the rotational g.s. sequence estimated in lighter isotopes (up to ≈ 157) is compatible with isomerism, for example, $\approx 0.6 - 0.8$ MeV in PNP/qp method for $N = 153$.

For larger N , the lowest excitation energies rise to ≈ 2 MeV at $N = 167$ in the PNP, and slightly less in the q.p. method. Again, the energy differences between two types of configurations are more pronounced in the PNP variant of calculations - see Fig. 7. The energies predicted by the quasiparticle method are generally slightly higher than those of the PNP in the $N < 151$ region, but lower than them for $N > 153$.

In summary, both methods identify Rf isotopes with $N \lesssim 155$, and particularly those around $N = 149 - 151$, as the most promising for low-lying $1\nu 2\pi$ isomers, with predicted excitation energies as low as 1.0–1.2 MeV.

The preceding discussion concerning even-odd Fm, No, and Rf isotopes changes if we

assume the inverted order of the proton $1/2_{10}^-$ and $7/2_3^-$ levels (cf Fig. 4), as it is suggested by the experimentally established spins of low-lying states in Md and Lr isotopes around $N = 150$ [89–91]. In such a case, the excitation of the proton $K_{2\pi} = 7$ pair in Fm isotopes would be smaller and the isomeric character of configurations including it more probable in lighter isotopes. In No, the inversion of these proton levels would make the $K_{2\pi} = 8$ proton pair optimal and would lower energies of high- K configurations involving it. The consequence for Rf isotopes would be an increase in energies of configurations including the $K_{2\pi} = 8$ proton pair and a decrease in those with the $K_{2\pi} = 5$ pair. Overall, prospects for high- K isomers in these nuclei would become more similar (this means, better in Fm and No), especially in lighter isotopes.

Sg Both in the PNP and quasiparticle calculations, the energetically favoured configurations contain the $\pi^2 7^- \{5/2_5^- \otimes 9/2_2^+\}$ pair (circles and squares in Fig 8) while the second lowest often involve the $\pi^2 6^+ \{5/2_5^- \otimes 7/2_3^-\}$ pair (triangles and diamonds), see also Fig. 4. Energies of the $1\nu 2\pi$ high- K states are the lowest for the lightest isotopes. In the PNP results, energies very slowly rise from ≈ 0.95 MeV at $N = 141$, attaining values $\approx 1.1 - 1.2$ MeV at $N = 151, 153$ and ≈ 1.25 MeV at $N=159$ (in the range of known isotopes); only for $N > 161$ they rise more, to ≈ 1.8 MeV at $N = 167$. The quasiparticle method (lower panel) gives qualitatively similar results, with slightly higher lowest energies for $N \leq 151$ isotopes, reaching minimum around 1.1 MeV.

Low energies obtained for configurations involving the $K_{2\pi} = 7$ pair up to $N=159$ translate to relatively low excitation above the g.s. rotational sequence and suggest their likely isomeric character. This makes Sg a promising element for a search of low-lying $1\nu 2\pi$ isomers.

Hs Energies of the lowest high- K $1\nu 2\pi$ configurations in Hs isotopes are larger than in Sg (except for the heaviest isotopes) as the 2p excitations involve the promotion of one proton above the $Z=108$ gap, see Fig. 4. The $1\nu 2\pi$ states which contain the proton pair $\pi^2 7^+ \{5/2_5^- \otimes 9/2_2^-\}$ are the lowest up to $N=151 - 153$ (Fig. 9, circles) while those with $\pi^2 8^- \{5/2_5^- \otimes 11/2_2^+\}$ (diamonds) become the lowest from $N = 153$ on. The lowest $1\nu 2\pi$ configuration for $N=169$ is $\nu 5/8_8^+ \otimes \pi^2 6^- \{11/2_1^+ \otimes 1/2_{10}^-\}$, at smaller deformation $\beta_{20} \approx 0.17$ and $E^* = 1.77$ MeV within PNP and 100 keV less in the q.p. method.

In the PNP formalism (upper panel), the lowest-lying states have energies 1.25–1.4 MeV for lighter isotopes ($N \leq 151$), and 1.5–1.6 MeV for $N = 153 - 165$. The estimate of

excitation above the g.s. rotational band in experimentally relevant isotopes $N \geq 153$ gives ≈ 0.7 and 1.1 MeV with the assumed $K_\nu = 11/2$ and $1/2$, respectively, so some of these configurations could be isomeric.

In the quasiparticle calculations (the lower panel) there is a smaller difference between two types of configurations; between $N = 141$ and 163 they remain in the range $1.3 - 1.45$ MeV. Since for $N \geq 153$ these energies are smaller than in the PNP method, and they provide even better case for isomerism.

While high- K isomers in Hs are possible, the higher excitation energies make them less favoured than in Rf and Sg.

Ds In this isotopic chain, energies of the lowest-lying high- K $1\nu 2\pi$ configurations are predicted smaller than for Hs. The lowest-energy proton-pair excitations are formed from orbitals situated above the $Z = 108$ shell gap, see Fig. 4. The energetically favoured $1\nu 2\pi$ high- K states contain the $\pi^2 10^- \{11/2_1^+ \otimes 9/2_2^-\}$ pair for $N \leq 159$, Fig 10 (circles, squares), and $\pi^2 7^- \{11/2_1^+ \otimes 3/2_8^-\}$ for $N \geq 161$ (diamonds, asterisks). Considering isotopes $N \geq 153$ (as lighter ones are experimentally inaccessible), the lowest PNP energies, $E_{\nu\pi^2}^* \approx 1.3$ MeV, are predicted around $N = 163$, see Fig. 10, upper panel. Especially configurations involving the $K_\pi = 10$ proton pair are good candidate for isomers (it is likely that the same two-proton pair is involved in the known isomer in ^{270}Ds).

The quasiparticle method (lower panel) also identifies a region of low energies around $N = 157$, with a minimum of about 1.25 MeV.

In PNP calculations for the $N=169$ isotope, $1\nu 2\pi$ configurations involving one of the following neutron levels: $11/2_2^+$, $5/2_8^+$ and $9/2_4^+$, all have similar energies, dependent primarily on the proton pair, with the lowest one for the $K_\pi = 10$ pair (Fig. 10, black square). A similar situation occurs in the $N = 171$ isotope, where the lowest-lying configurations are built from one of the neutron levels $5/2_8^+$, $3/2_{11}^+$, and $15/2_1^-$, coupled to the $\pi^2 6^- \{11/2_1^+ \otimes 1/2_{10}^-\}$ pair, with excitation energies of $E^* \approx 1.8$ MeV (Fig. 10, brown cross). The energy of configurations involving the $K_\pi = 10$ proton pair is ≈ 150 keV higher when coupled to lower- Ω_ν neutron states, and about ≈ 350 keV higher when coupled to the neutron $15/2_1^-$ state.

In summary, both approaches suggest that Ds isotopes are promising candidates for $1\nu 2\pi$ isomerism in the range $N = 155-161$, and somewhat less so (due to the smaller aligned $K_{2\pi}$ value) for $N = 163$.

Cn It can be seen in Figure 11 that in isotopes with $153 \leq N \leq 169$ the lowest-

lying configurations following from the PNP calculations contain the $\pi^2 6^+ \{9/2_2^- \otimes 3/2_8^-\}$ pair (diamonds and asterisks) while those with the $\pi^2 10^- \{11/2_1^+ \otimes 9/2_2^-\}$ pair lie ≈ 200 - 300 keV higher (very light isotopes probably are outside experimental possibilities). The lowest energies of $1\nu 2\pi$ states in the PNP calculation, $E^* \approx 1.35$ MeV, occur around $N=163$ (upper panel). Similar energies in the same range of isotopes are obtained in the quasiparticle calculations (lower panel). However, configurations involving two proton pairs are closer in energy in isotopes $N = 157 - 163$. The isomeric character of these states, although possible, is not certain as the $K_{2\pi} = 6$ of the aligned proton pair is not large as for their excitation energy.

In PNP calculations, the lowest energies of $1\nu 2\pi$ configurations in the $N=171, 173$ isotopes are around 2 MeV. The involved proton pairs are $\pi^2 9^- \{11/2_1^+ \otimes 7/2_4^-\}$ in $N=171$ and $\pi^2 10^- \{13/2_1^+ \otimes 7/2_4^-\}$ in $N=173$, which form configurations with similar energies when coupled to one of the neutrons states: $5/2_8^+$, $3/2_{11}^+$, $15/2_1^-$ (and $1/2_{15}^+$ in $N=173$). Energies from the qp calculations for $N = 171$ are smaller. In deciding whether these or the configurations in $N=171, 173$ isotopes of Ds could be isomeric, one has to take into account their reduced β_{20} deformations of $\approx 0.13 - 0.15$ ($N=171$) and $0.08 - 0.1$ ($N=173$). They imply moments of inertia substantially smaller than in lighter isotopes and, consequently, smaller excitation of the $3qp$ states above the g.s. rotational band. Therefore, in spite of relatively high energy, configurations with large $K_{2\pi}$ and K_ν may qualify as candidates for isomers.

In summary, for Cn isotopes, the prospects for finding low-lying $1\nu 2\pi$ isomers exist, but are weaker than in Rf and Sg due to higher energies and smaller aligned angular momentum $K_{2\pi}$ of the proton pair.

The calculated excitation energies for the lowest $1\nu 2\pi$ quasiparticle (q.p.) configurations, obtained using the quasiparticle method, are summarized in Figure 12. For the lighter elements in this study, specifically $Z = 100$ (Fm) and $Z = 102$ (No), the excitation energies are generally high, predominantly falling into the red ($E^* > 1.7$ MeV) and yellow ($1.5 < E^* < 1.7$ MeV) regions, and tend to increase with neutron number across the displayed range. In stark contrast, for $Z = 104$ (Rf) and $Z = 106$ (Sg), a significant region characterized by lower excitation energies (blue, $1.1 < E^* < 1.3$ MeV) is predicted across a broad range of neutron numbers, approximately $N = 145$ – 157 . Outside this blue region, energies for Rf and Sg generally increase, transitioning through green ($1.3 < E^* < 1.5$ MeV) to yellow and red at higher N values. For the heavier elements investigated, $Z = 108$ (Hs) and $Z = 112$

(Cn), the excitation energies are mostly found within the green range (1.3–1.5 MeV) and exhibit less pronounced systematic variation with N . It is noteworthy that for $Z = 110$ (Ds), while the energies are generally in the green region, a localized minimum (blue, 1.1–1.3 MeV) appears around $N = 163$. Consequently, the lowest excitation energies for these $1\nu 2\pi$ configurations, as calculated with the quasiparticle method, are predominantly found for Rf and Sg in the $N \approx 145$ –157 region, and for Ds in the vicinity of $N \approx 163$.

B. Excitation energies of 3-neutron q.p. high- K - candidates for isomeric states

Energies for selected, mostly low-lying 3-neutron q.p. configurations calculated within the PNP and quasiparticle methods are shown in Figs. 13-19. As mentioned in the previous section, the neutron pairing strengths fixed at the ratio $G_n(N, Z)/G_n^{mod}(N, Z) = 1.1$, with $G_n^{mod}(N, Z)$ the pairing strengths of our MM model, produced seemingly too low 3ν excitation energies in some nuclei. Therefore, we discuss results of the PNP calculations with stronger pairing, with the above ratios fixed at 1.15.

In each of these two methods, the lowest 3ν states were independently selected since (as already mentioned) differences in 3ν excitation energies are expected between the q.p. and PNP results, especially for $N = 151, 153$ and $N = 161, 163$ around the large gaps in the neutron s.p. spectrum. Results of the q.p. method in Figs. 13-19 were obtained by taking the even-even core with the neutron number $N - 1$. In comparison with the other version, with the core of N neutrons, its results are closer to those of PNP for $N = N_{gap} + 1$, while they remain unphysical for $N_{gap} - 1$.

Energies $E_{\nu 3}^*$ are presented in Figures 13-19 for isotonic sequences vs Z . Those of the q.p. method (in lower panels) are shown for 3ν configurations that come out the lowest in some isotone. The PNP results (in upper panels) are also shown for isomer candidates that are lying somewhat higher, with a favourable relation of energy to K . We also show energies for some configurations for which the two methods differ substantially. Configurations are distinguished by the shapes of the points they are plotted with (those occurring in both panels have the same marker). Colours of displayed points refer to the isotonic chain.

Isotones $N=143, 145$ The low-lying high- K 3ν configurations in these isotones have to contain at least two of the $\nu 5/2_7^+, \nu 5/2_7^-, \nu 7/2_5^-$ or $\nu 7/2_4^+$ orbitals - see Fig. 3.

In the q.p. method, the configurations composed of $\nu 5/2_7^- \otimes \nu 7/2_5^-$ and either $\nu 1/2_{13}^+$ or

$\nu 1/2_{13}^-$ neutron states are the lowest in lighter $N = 143$ isotones (black squares and crosses in the lower panel of Fig. 13). The configuration with $\nu 5/2_7^+$ instead of $\nu 5/2_7^-$ lies ≈ 200 keV higher (black asterisk in the lower panel of Fig. 13). In the $N = 145$ isotones, the lowest configuration is $\nu^3\{1/2_{13}^+ \otimes 5/2_7^+ \otimes 7/2_5^-\}$, at $\approx 1.3 - 1.5$ MeV in Fm, No, and Rf (red circles in the lower panel of Fig. 13).

Results of the PNP method are similar, with the same lowest configuration in $N = 145$ isotones (upper panel of Fig. 13). The lowest PNP 3ν configurations in $N = 143$ have the $\nu 5/2_7^-$ neutron replaced with $\nu 5/2_7^+$ (black circles and asterisks).

As the energies of one-neutron states $\nu 7/2_5^-$, $\nu 1/2_{13}^+$, $\nu 1/2_{13}^-$ are close to each other, within < 100 keV in lighter $N = 143, 145$ isotones, energies of 3ν configurations containing them should be considered relative to those of the collective band built on the $\nu 7/2_5^-$ level. Then, the excitation energy of, for example, the $\nu^3\{7/2_5^- \otimes 1/2_{13}^+ \otimes 5/2_7^+\}$ configuration should be compared to the rotational energy corresponding to 3 ($1/2 + 5/2$) \hbar units of the collective angular momentum. The latter value is much smaller than the former, so a large hindrance of the decay of the lowest 3ν configuration to this band is not expected.

Therefore, we also show energies of $\nu^3\{7/2_5^- \otimes 7/2_4^+ \otimes 5/2_7^\pm\}$ configurations with larger $K = 19/2$ (black triangles and red inverted triangles in upper panel, Fig. 13). However, even the lower one, at ≈ 2 MeV in $N=145$ isotones, still has estimated excitation above the collective rotational band of more than 1 MeV.

In summary, configurations with the same K lie lower in light $N = 145$ isotones and have a better chance of being isomeric there. However, due to $\gtrsim 1$ MeV excitation over low-lying rotational 1ν band, there are no prominent candidates for 3ν high- K isomers in $N = 143, 145$ isotones.

Isotones $N=147, 149$ The configuration of three states below the $N=152$ gap, $\nu^3\{9/2_3^- \otimes 7/2_4^+ \otimes 5/2_7^+\}$, is a candidate for an isomer in $N = 149$ isotones (red squares in Fig. 14). As the g.s. K values predicted for $N=149$ are either $7/2$ or $9/2$ (cf Fig. 2), the extra aligned angular momentum projection is either 7 or 6 \hbar units relative to the g.s. rotational bands. From energies $\approx 1.2 - 1.3$ MeV in the q.p. method, and more varied $1.1 - 1.7$ MeV in the PNP, we estimate the excitation energy of 0.6 - 0.7 MeV above g.s. rotational band in No and slightly smaller (larger) in Rf in the q.p. (PNP) method. The configuration with K larger by one (red diamonds in upper panel of Fig. 14) lies already ≈ 0.5 MeV higher which makes it much worse candidate for an isomer.

The lowest configurations for $N = 147$ in the q.p. calculations contain the $\nu 1/2_{13}^+$ state (black triangles and inverted triangles in the lower panel of Fig. 14). As the predicted g.s. K -values for $N = 147$ isotones are either $5/2$ or $7/2$ (Fig. 2), with only 3 or 4 units of extra aligned- K and excitation energy of ≈ 1.5 MeV, these are not the best candidates for isomers. Therefore, we show PNP results for other, higher- K states (upper panel of Fig. 14): one that is the lowest for $N = 149$ (black squares) and the $K = 19/2$ configuration with $\nu 7/2_5^-$ and $\nu 7/2_4^+$ neutrons (black dots). With extra aligned K of 7 and 8 relative to the $K=5/2$ g.s. in Fm and No, they are not excluded as candidates for isomerism, although less favoured than the one in $N = 149$.

Isotones $N=151, 153$ In q.p. calculations, the lowest 3ν energies in $N = 151$ isotones are obtained for configurations built of neutron orbitals below the $N = 152$ gap (black squares and circles in the lower panel of Fig. 15). As discussed earlier, this results from an improper position of the Fermi energy in the q.p. formalism. In the PNP calculations, the same configurations lie much higher (black squares, upper panel). The effect of the $N = 152$ gap in the PNP calculation makes energies of all 3ν states are rather high. For example, the configuration $\nu^3\{11/2_2^- \otimes 9/2_3^- \otimes 7/2_4^+\}$ with extra 9 \hbar units of K relative to the g.s. (which is predicted as the $\nu 9/2_3^-$ state - cf Fig. 2) has energy above 2 MeV in PNP calculations (black triangles in the upper panel). This corresponds to $\approx 1.4(1)$ MeV estimated excitation above the g.s. rotational band in Fm (Sg), which seems large for an isomer.

Calculated energies of low-lying 3ν configurations in $N=153$ isotones are greater than 1.8 (1.7) MeV in the q.p. (PNP) method. The similarity of the q.p. results to those of the PNP follows from the choice of the $N - 1 = 152$ system as the core: pairing Fermi energy is situated in the middle of the $N = 152$ gap, hence energies of quasiparticles from below the gap are not so underestimated as for $N = 151$. At large excitation energies, interesting configurations with large extra aligned K relative to the low-lying 1ν bandheads with $K = 1/2$ (g.s.), $3/2$ and $11/2$. The PNP energies for the $\nu^3\{\nu 11/2_2^- \otimes \nu 9/2_3^- \otimes \nu 1/2_{14}^+\}$ and $\nu^3\{\nu 11/2_2^- \otimes \nu 9/2_3^- \otimes \nu 7/2_5^+\}$ configurations are shown in Fig. 15 (upper panel, red inverted triangles and pentagrams). Since the $K = 11/2$ band head lies only ≈ 200 keV above the $K = 1/2$ g.s. in Fm and becomes the g.s. in Ds and Cn, crucial are the excitation energies of these 3ν states relative to the rotational states with $I = K_{\nu^3}$ built on the $K = 11/2$ and $K = 1/2$ band heads. The estimated values of those in Fm - Sg are: ≈ 1.1

MeV for the $K = 21/2$ configuration (roughly the same relative to both band heads) and ≈ 1 MeV for the $K = 27/2$ one - not excluding, but not favouring their isomerism either.

Isotones $N=155, 157$ Low-lying 3ν states in these isotones are built from neutron orbitals above the $N = 152$ gap. Ground states predicted within the q.p. method are formed by the $1/2_{14}^+$ (in Fm - Hs) and $11/2_2^-$ (in Ds, Cn) orbitals (cf Fig. 2). These two 1ν configurations and the one built on the $\nu 3/2_{10}^+$ level lie very close to each other in $N = 155, 157$ isotones (within less than 100 keV, often nearly degenerate). In $N = 157$ isotones, additionally $\nu 7/2_5^+$ and $9/2_3^+$ states lie very close to the above (this relates to differences between the PNP and q.p. predictions for g.s. configurations in $N=157$ isotones - cf Fig. 2).

In the q.p. method, the lowest 3ν configuration in both isotone chains is $\nu^3\{11/2_2^- \otimes 1/2_{14}^+ \otimes 3/2_{10}^+\}$ at $E_{\nu^3}^* < 1.5$ MeV, with lower energies for $N = 157$ (black and red circles in the lower panel of Fig. 16). In the PNP method, this configuration lies very low in $N = 155$ isotones. Above it, at $E_{\nu^3}^* \approx 1.5$ MeV, there are two states $\nu^3\{11/2_2^- \otimes 7/2_5^+ \otimes 1/2_{14}^+(3/2_{10}^+)\}$, one of which is shown in Fig. 16 (black triangles); at $E_{\nu^3}^* \approx 2$ MeV lie two other 3ν states: $\nu^3\{11/2_2^- \otimes 9/2_3^+ \otimes 3/2_{10}^+\}$ and $\nu^3\{11/2_2^- \otimes 9/2_3^+ \otimes 7/2_5^+\}$ (black inverted triangles and diamonds). Estimated excitation of these states above the rotational band built on the $K = 11/2$ band head (at their respective angular momentum values) are $\approx 0.9 - 1, 1.1$ and 1.2 MeV, respectively, for the $K = 15/2, 19/2$, and $27/2$ configurations.

In the PNP calculations for $N = 157$ isotones, the $\nu^3\{11/2_2^- \otimes 1/2_{14}^+ \otimes 3/2_{10}^+\}$ configuration is not the lowest one; its energy (not shown in Fig. 16) is similar as those of two other configurations: $\nu^3\{11/2_2^- \otimes 7/2_5^+ \otimes 3/2_{10}^+\}$ and $\nu^3\{11/2_2^- \otimes 9/2_3^+ \otimes 7/2_5^+\}$ (red inverted triangles and diamonds in the upper panel of Fig. 16). The configurations $\nu^3\{11/2_2^- \otimes 7/2_5^+ \otimes 1/2_{14}^+(3/2_{10}^+)\}$ lie lower, at $\approx 1.3 - 1.5$ MeV (red squares and triangles in the upper panel of Fig. 16). These four configurations lie lower than in $N = 155$ isotones. Their excitation above the $K=11/2$ g.s. rotational band amounts to ≈ 0.8 MeV for the $\nu^3\{11/2_2^- \otimes 7/2_5^+ \otimes 3/2_{10}^+\}$ state and ≈ 0.9 MeV for the $K = 27/2$ configuration - so they are likely candidates for isomers.

Isotones $N=159, 161, 163$ Energies of low-lying high- K configurations in $N=159$ - 163 even-odd isotones are depicted in Fig. 17, 18. The ground states of these nuclei are predicted by the q.p. calculation are mostly formed by the $7/2_4^+, 9/2_3^+$ and (exclusively) $13/2_1^-$ neutron states for $N=159, 161, 163$, respectively, while in the PNP method, one often

obtains the $K^\pi = 9/2^+$ g.s. in $N = 159$ isotones (cf Fig 2).

Low-lying 3ν states in $N = 159$ isotones are built from neutron orbitals below the $N = 162$ gap. The best candidate for isomer seems to be the $\nu^3\{11/2_2^- \otimes 9/2_3^+ \otimes 7/2_5^+\}$ configuration, at $E_{\nu^3}^* \approx 1.3\text{-}1.5$ MeV in the PNP calculations, and 1.2 - 1.3 MeV in the q.p. method (black squares in Fig. 17), with an extra 9 or 10 \hbar units of K with respect to the g.s. (which has $K = 7/2$ or $9/2$ - Fig. 2). Its excitation above the same spin state of the g.s. rotational band is estimated as 0.3 - 0.4 MeV for ^{263}Rf . For the Ds and Cn, the configuration $\nu^3\{3/2_{10}^+ \otimes 9/2_3^+ \otimes 7/2_5^+\}$ lies lower, but has smaller K .

The same configuration as in $N = 159$ is favoured for $N = 161$ isotones within the q.p. method. In the PNP calculation, which accounts for proper position of the Fermi energy, it is highly excited as all three states lie below the $N=162$ gap (red squares in Fig. 17). The more interesting is the optimal configuration $\nu^3\{13/2_1^- \otimes 9/2_3^+ \otimes 7/2_5^+\}$ (red diamonds in Fig. 17) that has K by 10 units of \hbar bigger than the g.s. and energy $E_{\nu^3}^* = 1.7 - 2$ MeV, decreasing with Z . Its estimated excitation above the g.s. rotational band at spin $I = 29/2$ is ≈ 0.7 MeV in ^{265}Rf and less than that in Ds and Cn. It seems a very good candidate for the higher-lying high- K isomer.

Excitation energies of high- K 3ν configurations in $N=163$ isotones are mostly greater than 2 MeV in both variants of calculations (due to the choice of $N-1$ system as a core in the q.p. method) - Fig. 18. Still, for example, the energy of the configuration $\nu^3 33/2^+ \{13/2_1^- \otimes 11/2_2^- \otimes 9/2_3^+\}$ (triangles, lower panel) is underestimated by the q.p. method by 0.5 - 1.2 MeV compared to the more reliable PNP calculation. Out of two lowest-lying high- K 3ν configurations obtained in the PNP method, shown in Fig. 18, the more interesting is the one with higher K , $\nu^3 31/2^- \{13/2_1^- \otimes 9/2_4^+ \otimes 9/2_3^+\}$ (squares, upper panel). It would lie at an estimated ≈ 1 MeV above the same spin state of the g.s. rotational band built on the predicted $K = 13/2$ ground state. While such excitation is not small, this configuration could be a higher-lying, very high- K isomer.

Isotones $N=165$, 167 Ground states in $N = 165$ isotones are formed mostly by the $13/2_1^-$ orbital, while the 1ν $9/2_4^+$ and $3/2_{11}^+$ configurations lie close to it for, respectively, lighter and heavier isotones. For $N = 167$ situation is even more complicated as closely lying 1ν states: $11/2_2^+$, $9/2_4^+$, $3/2_{11}^+$ and $5/2_8^+$ compete to become the g.s., with $13/2_1^-$ state lying close (within 150 keV) up to $Z = 106$.

The same high- K 3ν configurations: $\nu^3\{13/2_1^- \otimes 5/2_8^+ \otimes 3/2_{11}^+\}$ and $\nu^3\{13/2_1^- \otimes 9/2_4^+ \otimes$

$3/2_{11}^+$ come out as the lowest-lying in both isotone chains in the q.p. calculation (black and red circles and triangles, lower panel of Fig. 19). In the PNP calculation, these configurations are also the lowest in $N = 165$ isotones (with energies 200-300 keV lower than the q.p. results). In Fig. 19 we also show energies for $\nu^3\{13/2_1^- \otimes 11/2_2^+ \otimes 9/2_4^+\}$ and $\nu^3\{13/2_1^- \otimes 9/2_4^+ \otimes 5/2_8^+\}$ states in $N = 165$ nuclei (black inverted triangles and squares, upper panel of Fig. 19).

For $N = 167$, PNP energies of configurations favoured in the q.p. calculations are much higher, nearly equal to those of the $\nu^3\{13/2_1^- \otimes 9/2_4^+ \otimes 5/2_8^+\}$ state, shown in Fig. 19 (red squares, upper panel). Configurations that come out lower in the PNP method are: $\nu^3\{9/2_4^+ \otimes 5/2_8^+ \otimes 3/2_{11}^+\}$ and $\nu^3\{11/2_2^+ \otimes 9/2_4^+ \otimes 3/2_{11}^+\}$ (red diamonds and asterisks, upper panel, Fig. 19). Thus, the q.p. and PNP results suggest a better chance for isomers in different isotonic chains.

For PNP results, estimates of the excitation above the g.s. rotational band are as follows. For $N = 165$, with the $K = 13/2$ g.s., the lowest two 3ν states have extra K of 4 or 6 \hbar units. Collective rotation reduces excitation $E_{\nu^3}^*$ for Hs by, respectively, 0.45 and 0.7 MeV, to ≈ 0.8 MeV in both cases. For the configuration with the highest $K = 33/2$ (black inverted triangles), with extra 10 \hbar units of K , the estimate for Hs gives ≈ 0.5 MeV above the g.s. band. This makes all these states, and especially one with the highest- K , good candidates for isomers. The 3ν states in $N = 167$ isotones lie higher than in $N = 165$, but still some of them can be isomeric.

Isotones $N=169, 171, 173$ In $N = 169$ isotones of Hs - Cn the 1ν states formed by the $9/2_4^+$ and $11/2_2^+$ orbitals are within a few tens of keV from the ground state. In Ds and Cn nuclei with $N = 171, 173$, their smaller equilibrium deformations β_{20} make a unique $15/2_1^-$ orbital equally close to the neutron Fermi level. Therefore one should expect very low-lying high- K 1ν isomers (or ground states, as the energy differences of 10 - 30 keV between 1ν configurations in the PNP calculation cannot be treated as absolutely certain) in these nuclei.

The lowest-lying high- K 3ν configurations in $N=169 - 173$ isotones are: $\nu^3 25/2^+ \{5/2_8^+ \otimes 11/2_2^+ \otimes 9/2_4^+\}$ at $E^* \approx 1.45$ MeV for $N=169$ in Hs, Ds and Cn, $\nu^3 23/2^- \{5/2_8^+ \otimes 15/2_1^- \otimes 3/2_{11}^+\}$ at $E^* \approx 1.3$ (1.25) MeV for $N=171$ in Ds (Cn) and $\nu^3 21/2^- \{5/2_8^+ \otimes 15/2_1^- \otimes 1/2_{15}^+\}$ at $E^*=1.36$ MeV for the $N=173$ isotone of Cn. To appreciate whether there is a hindrance of their decay to lower-lying collective structures one should consider rotational bands built

on the high- K 1ν band heads.

Considering the abovementioned 3ν configuration in $N = 169$ isotones, the extra-aligned K with respect to the low-lying band built on the $\nu 11/2_2^+$ state of $7 \hbar$ units points to ≈ 0.6 MeV of excitation over the collective structure and a good chance for isomerism. Regarding 3ν configurations in $N = 171, 173$ nuclei one encounters two counteracting circumstances: 1) their extra-aligned K with respect to the low-lying 1ν band built on the $\nu 15/2_1^-$ state, of 4 and 3 \hbar , respectively, is not large, 2) a reduced deformation β_{20} increases rotational energies. As the energies of these 3ν configurations are rather low, we expect that they also have a quite good chance of being isomeric.

C. Comparison with experimental evidence

Regarding a comparison of the above results with the experimental evidence, one can start with the very low-lying $11/2^-$ isomers found in ^{253}Fm (at ≈ 350 keV) [16], ^{255}No (at 240-300 keV [17] or 225 keV [18]) and ^{257}Rf (at ≈ 75 keV) [23], attributed to the $\nu 11/2_2^-$ [725] s.p. state. In the PNP calculation we obtain for those nuclei the following excitation energies of this configuration: 280, 240 and 180 keV, in a reasonable agreement with the data.

Two 3qp isomers were reported in $N = 149$ isotones: in ^{251}No ($\approx 2\mu\text{s}$, at > 1.7 MeV) [13, 19] and in ^{253}Rf (0.66 ms at $\gtrsim 1.02$ MeV [19] or $\approx 0.6 \mu\text{s}$ [20]). In the q.p. method, the $1\nu 2\pi$ excitations in ^{251}No including the lowest neutron $7/2_4^+$ state have the following energies and proton contents: 1.467 MeV $\pi^2\{9/2_2^+ \otimes 1/2_{10}^-\}$, 1.554 MeV $\pi^2\{9/2_2^+ \otimes 7/2_3^-\}$, and 1.807 MeV $\pi^2\{7/2_3^+ \otimes 7/2_3^-\}$. The 3 q.p. configurations with the neutron state changed to $\nu 9/2_3^-$ and $\nu 5/2_7^+$ lie ≈ 10 and 70 keV above them, respectively. In the PNP calculations, the energy 1.442 MeV of the lowest configuration is similar to the above, but that of the one with the $\pi^2 8^-$ pair is higher, $E^* = 1.85$ MeV. The lowest 3ν q.p. state in ^{251}No , $\nu^3\{9/2_3^- \otimes 7/2_4^+ \otimes 5/2_7^+\}$, has even lower energy: 1.172 MeV in the q.p. method and 1.149 MeV in PNP (red squares in Fig. 14). The two lowest $1\nu 2\pi$ configurations in ^{253}Rf obtained within the q.p. method contains the proton $\pi^2 8^- \{9/2_2^+ \otimes 7/2_3^-\}$ pair and either $\nu 9/2_3^-$ at 1.222 MeV or $\nu 7/2_4^+$ at 1.247 MeV; the PNP energies of those states are: 1.013 and 1.093 MeV, respectively. The same as in ^{251}No lowest 3ν configuration is calculated at 1.222 MeV in the q.p. method and at 1.295 MeV in PNP. From the above results, one would expect in ^{251}No an isomer at energy significantly lower than 1.7 MeV, whereas calculated energies of

$1\nu 2\pi$ and 3ν isomers in ^{253}Rf roughly agree with the one suggested in [19].

In $N = 151$ isotones, one 3q.p. isomer ($I \geq 23/2$, 0.63 ms, $E^* > 1.44$ MeV) is known in ^{253}No [14–16] and two ($I^\pi = 19/2^+$, 29 μs , $E^*=1.103$ MeV and $I^\pi = 25/2^+$, 49 μs , $E^*=1.303$ MeV) in ^{255}Rf [21, 22]. The isomer in ^{253}No is attributed either to one of the $\nu^3\{9/2_3^- \otimes 7/2_4^+ \otimes 7/2_5^+\}$ or $\nu^3\{9/2_3^- \otimes 5/2_7^+ \otimes 7/2_5^+\}$ structures [14], or to the neutron $9/2^-$ [734] state coupled to two-proton $\pi^2\{9/2^+[624] \otimes 7/2^-[514]\}$ configuration [15, 16]. Two isomers in ^{255}Rf are attributed to the neutron state $9/2^-$ [734] coupled with the $\pi^2\{9/2^+[624] \otimes 1/2^-[521]\}$ and $\pi^2\{9/2^+[624] \otimes 7/2^-[514]\}$ proton pair [21, 22]. Results of our calculations point to their $1\nu 2\pi$ rather than 3ν structure, as follows from the PNP results, more reliable for $N=151$. In particular, the calculated energy for the candidate 3ν state $\nu^3\{9/2_3^- \otimes 7/2_4^+ \otimes 7/2_5^+\}$ in ^{253}No is above 2 MeV (cf also neutron levels for ^{253}No in Fig. 3). Thus, the likely structure of these isomers seems to be as suggested in [22] for ^{255}Rf . Calculated energies of both $1\nu 2\pi$ configurations in ^{253}No are somewhat high: 1.44 and 1.89 MeV (in the PNP method), and 1.44 and 1.53 MeV (in the quasiparticle method). In ^{255}Rf , their energies: 1.026 and 1.434 MeV (in PNP), or 1.20 and 1.425 MeV (in the q.p. method) well agree with the data. However, the main problem in ^{255}Rf is the unlikely higher position of the state containing the $K_{2\pi} = 5$ proton pair relative to that with the $K_{2\pi} = 8$.

In $N = 153$ isotones, two 3q.p. isomers are known in ^{255}No ($I = 19/2 - 23/2$ at 1.4 - 1.6 MeV and $I \geq 19/2$ at ≥ 1.5 MeV according to [17] or $I^\pi = 21/2^+$ at ≈ 1.36 MeV and $27/2^+$ at ≈ 1.5 MeV according to [18]) and one (106 μs , $I^\pi = 21/2^+$ at 1.151 MeV [23–25]) in ^{257}Rf . The structure suggested for two ^{255}No isomers in [18] is: $\nu 11/2^-$ [725] state coupled to $\pi^2\{1/2^-[521] \otimes 9/2^+[624]\}$ and $\pi^2\{7/2^-[514] \otimes 9/2^+[624]\}$. The isomer in ^{257}Rf was attributed to the first of the above configurations [23, 25]. Based on our results, 3ν states in $N = 153$ isotones have energies greater than 1.7 MeV (Fig. 14). Among predicted $1\nu 2\pi$ configurations, the candidates suggested in [18] for ^{255}No come out at 1.74 and 2.12 MeV in PNP calculations (1.67 and 1.74 MeV in the quasiparticle method), which is too high. In ^{257}Rf , as in ^{255}Rf , the suggested configuration is predicted unnaturally above the one with the $K_\pi = 8$ pair: the energy of the latter is 1.24 MeV in PNP and 1.36 in the q.p. method, while that of the former is 1.63 MeV in PNP and 1.59 MeV in the q.p. method.

A better agreement with experiment for $N=151$ and 153 isotones of No and Rf could be reached by taking into account the inverted order of proton $1/2_{10}^-$ and $7/2_3^-$ levels. As argued in the discussion of $1\nu 2\pi$ results, such a change, including a smaller gap between these two

levels than in the present Woods-Saxon spectrum would lead to a smaller energy difference between configurations including $K_\pi=5$ and 8 proton pairs and lower energies of $1\nu 2\pi$ states in No isotopes.

IV. CONCLUSIONS

This work presents a systematic theoretical search for possible three-quasiparticle ($1\nu 2\pi$ and 3ν) high- K isomers in even-odd Fm–Cn nuclei within a Microscopic-Macroscopic model with the deformed Woods-Saxon potential [59].

We performed two sets of calculations differing in the treatment of pair correlations: one using the quasiparticle method and the other using the particle number projection. Both give similar results for excitation energies of $1\nu - 2\pi$ high- K states and point to mostly the same configurations as candidates for isomers. Deficiencies of the simpler quasiparticle approach show up in calculated excitation energies of 3ν states, which are particularly unreliable for non-optimal configurations at neutron numbers close to the large gaps in the single-particle spectrum, i.e., for $N = N_{\text{gap}} \pm 1$ (where N_{gap} denotes the gap position).

Candidates for three-quasiparticle (3q.p.) high- K isomers were selected on the basis of their low excitation energy and the small estimated energy above the collective rotational sequence built on the one-quasiparticle (1q.p.) band head. The latter involves one of its components (the 1ν state in the case of $1\nu - 2\pi$ configurations, or any of the three 1ν states in the case of the 3ν configuration). The second estimate, based on cranking calculations [68], is rather schematic, a limitation dictated by the scarcity of available experimental data.

The most promising candidates for high- K $1\nu - 2\pi$ isomers, with excitation energies as low as ≈ 1.0 MeV, are predicted in Rf ($Z = 104$) and Sg ($Z = 106$) isotopes for neutron numbers up to $N \approx 159$. Relatively low-energy candidates occur in Ds around $N = 163$ and, with slightly higher energy and higher K , for $N = 157$ – 161 .

(involving the $K_{2\pi} = 10$ proton pair). In Hs ($Z = 108$), where the proton gap increases the lowest excitation energies, and in experimentally accessible Cn nuclei, with configurations having moderate aligned $K_{2\pi} = 6$, isomerism is possible. In No nuclei, best candidates occur for $N = 149 - 155$, while there are not many candidates in Fm.

Best candidates for the 3ν high- K isomers following from the more reliable PNP results occur in isotones $N = 149, 157, 159$ and 165 . The energy penalty for promoting a

neutron pair across the $N = 152$ or $N = 162$ gap rises energies of 3ν configurations in $N = 151, 153, 161$ and 163 isotones. However, for $N = 161$ and 163 , our model predicts higher-lying configurations with $K \approx 15$, which could have some hindrance to EM decay. Furthermore, for the heaviest isotopes ($N \geq 169$), relatively small excitation energies and reduced quadrupole deformation which increases rotational energies, could create conditions for isomeric state.

Comparisons of our results with available experimental data on ground states, 1 q.p. and 3q.p. isomers (in No and Rf isotopes) show some agreement but also some differences. In particular, seemingly contrary to evidence, the calculation predicts the $1\nu 2\pi$ state with the $K_{2\pi} = 5$ proton pair above the one with the $K_{2\pi} = 8$ one in $^{255,257}\text{Rf}$, the reported g.s. in ^{259}No has spin/parity $9/2^+$ vs the predicted $11/2^-$, and the calculated position of the $1\nu 2\pi$ configurations with the neutron $11/2^- [725]$ orbital in ^{255}No and ^{257}Rf is higher than suggested by their isomeric attribution. As discussed in the text, a part of these discrepancies may result from the relative position of proton $1/2_{10}^-$ and $7/2_3^-$ orbitals in our Woods-Saxon potential.

In conclusion, in view of the structure of the deformed mean field in superheavy nuclei it is nearly certain that high- K isomers will be found in many even-odd isotopes of the studied region. Predictions of our MM model will be confronted with forthcoming experimental results and in this way, many features will be tested. In particular, the presence of the $N = 152$ and $N = 162$ gaps in the s.p. neutron spectrum would be incompatible with the existence of low-lying 3ν isomers in $N = 151, 152, 161$, and 163 isotones. This and other questions await resolution, and this emphasizes the need for new data to test and constrain the fundamental aspects of nuclear models.

ACKNOWLEDGEMENTS

M. K. was co-financed by the International Research Project COPIGAL.

-
- [1] P. Walker and G. Dracoulis, *Nature* **399**, 35 (1999).
 - [2] J. Khuyagbaatar, *EPJ Web Conf.* **163**, 00030 (2017).
 - [3] A. Lopez-Martens *et al.*, *Eur. Phys. J. A* **58**, 134 (2022).

- [4] R. D. Herzberg and P. Greenlees, Prog. Part. Nucl. Phys. **61**, 674 (2008).
- [5] F. G. Kondev *et al.*, At. Data Nucl. Data Tables **103-104**, (2015).
- [6] P. M. Walker and F. R. Xu, Phys. Scr. **91**, 013010 (2016).
- [7] A. Ghiorso *et al.*, Phys. Rev. C **7**, 2032 (1973).
- [8] S. K. Tandel *et al.*, Phys. Rev. Lett. **97**, 082502 (2006).
- [9] R. D. Herzberg *et al.*, Phys. Rev. Lett. **97**, 082502 (2006).
- [10] R.-D. Herzberg *et al.*, Nature **442**, 996 (2006).
- [11] F. P. Heßberger *et al.*, Eur. Phys. J. A **43**, 55 (2010).
- [12] R. M. Clark *et al.*, Phys. Lett. B **690**, 19 (2010).
- [13] F. P. Hessberger *et al.*, Eur. Phys. J. A **30**, 561 (2006)
- [14] A. Lopez-Martens *et al.*, Eur. Phys. J. A **32**, 245 (2007)
- [15] B. Streicher *et al.*, Eur. Phys. J. A **45**, 275 (2010)
- [16] S. Antalic *et al.*, Eur. Phys. J. A **47**, 62 (2011)
- [17] A. Bronis *et al.*, Phys. Rev. C **106**, 014602 (2022).
- [18] K. Kessaci *et al.*, Phys. Rev. C **110**, 054310 (2024)
- [19] A. Lopea-Martens *et al.*, Phys. Rev. C **105**, L021306 (2022).
- [20] J. Khuyagbaatar *et al.*, Phys. Rev. C **104**, L031303 (2021).
- [21] P. Mosat *et al.*, Phys. Rev. C **101**, 034310 (2020).
- [22] R. Chakma *et al.*, Phys. Rev. C **107**, 014326 (2023).
- [23] J. S. Berryman *et al.*, Phys. Rev. C **81**, 064325 (2010)
- [24] J. Qian *et al.*, Phys. Rev. C **79**, 064319 (2009)
- [25] J. Rissanen *et al.*, Phys. Rev. C **88**, 044313 (2013)
- [26] D. Ackermann, S. Antalic, and F. P. Hessberger, Eur. Phys. J. Spec. Top. **233**:1017 (2024).
- [27] D. Ackermann, arXiv:2501.04053v1
- [28] F. G. Kondev, M. Wang, W. J. Huang, S. Naimi, and G. Audi, Chinese Physics C **45**, 030001 (2021)
- [29] A. P. Robinson *et al.*, Phys. Rev. C **78**, 034308 (2008).
- [30] B. Sulignano *et al.*, Phys. Rev. C **86**, 044318 (2012).
- [31] J. Kallunkathariyil *et al.*, Phys. Rev. C **101**, 011301(R) (2020).
- [32] D. Peterson *et al.*, Phys. Rev. C **74**, 014316 (2006).
- [33] H. M. David *et al.*, Phys. Rev. Lett. **115**, 132502 (2015).

- [34] K. Hauschild *et al.*, Phys. Rev. C **78**, 021302(R) (2008).
- [35] S. Antalic *et al.*, Eur. Phys. J. A **38**, 219 (2008).
- [36] H.B. Jeppesen *et al.*, Phys. Rev. C **80**, 034324 (2009).
- [37] T. Goigoux *et al.*, Eur. Phys. J. A **57**, 321 (2021).
- [38] A. Chatillon *et al.*, Eur. Phys. J. **30**, 397 (2006).
- [39] M. Asai, F.P. Heßberger, and A. Lopez-Martens, Nucl. Phys. A **944** (2015).
- [40] R. Briselet *et al.*, Phys. Rev. C **102**, 014307 (2020).
- [41] A. Lopez-Martens and K. Hauschild, Eur. Phys. J. A **58**(7), 134 (2022).
- [42] F. Heßberger *et al.*, Eur. Phys. J. A **12**, 57 (2001).
- [43] D. Ackermann, Nucl. Phys A **944** (2015).
- [44] G. D. Dracoulis, P. M. Walker, and F. G. Kondev, Rep. Prog. Phys. **79**, 076301 (2016).
- [45] P. Walker and Z. Podolyák, Phys. Scr. **95**, 044004 (2020).
- [46] P. T. Greenlees *et al.*, Phys. Rev. C **78**, 021303(R) (2008).
- [47] H. L. Liu, P. M. Walker, and F. R. Xu, Phys. Rev. C **89**, 044304 (2014).
- [48] R.-D. Herzberg *et al.*, Phys. Rev. C **65**, 014303 (2001).
- [49] S. Ketelhut *et al.*, Phys. Rev. Lett. **102**, 212501 (2009).
- [50] S. Eeckhaudt *et al.*, Eur. Phys. J. A **26**, 227 (2005).
- [51] P. T. Greenlees *et al.*, Phys. Rev. Lett. **109**, 012501 (2012).
- [52] S. Ówiok, J. Dudek, W. Nazarewicz, J. Skalski, and T. Werner, Comput. Phys. Commun. **46**, 379 (1987).
- [53] H. J. Krappe, J. R. Nix, and A. J. Sierk, Phys. Rev. C **20**, 992 (1979).
- [54] I. Muntian, Z. Patyk, and A. Sobiczewski, *Acta Phys. Pol. B* **32**, 691 (2001).
- [55] M. Kowal, P. Jachimowicz, and A. Sobiczewski, *Phys. Rev. C* **82**, 014303 (2010).
- [56] P. Jachimowicz, M. Kowal, and J. Skalski, *Phys. Rev. C* **89**, 024304 (2014).
- [57] P. Jachimowicz, M. Kowal, and J. Skalski, *Phys. Rev. C* **85**, 034305 (2012); *Phys. Rev. C* **101**, 014311 (2020).
- [58] P. Jachimowicz, M. Kowal, and J. Skalski, *Phys. Rev. C* **95**, 014303 (2017).
- [59] P. Jachimowicz, M. Kowal, and J. Skalski, *Atomic Data and Nuclear Data Tables* **138**, 101393 (2021).
- [60] V. N. Fomenko, J. Phys. A **3**, 8 (1970)
- [61] P. Jachimowicz, M. Kowal, and J. Skalski, *Phys. Rev. C* **108**, 064309 (2023).

- [62] S. wiok and S. Hofmann, *Nucl. Phys. A* **573**, 356 (1994).
- [63] A. Parkhomenko and A. Sobiczewski, *Acta Phys. Pol. B* **35**, 2447 (2004); *Acta Phys. Pol. B* **36**, 3115 (2005).
- [64] Z. Patyk and A. Sobiczewski, *Nucl. Phys. A* **533**, 132 (1991).
- [65] Z. Patyk and A. Sobiczewski, *Phys. Lett. B* **256**, 307 (1991).
- [66] H. L. Liu, F. R. Xu, P. M. Walker, and C. A. Bertulani, *Phys. Rev. C* **83**, 011303(R) (2011).
- [67] N. Minkov, L. Bonneau, P. Quentin, J. Bartel, H. Molique, and D. Ivanova, *Phys. Rev. C* **105**, 044329 (2020).
- [68] A. Sobiczewski, I. Muntian, and Z. Patyk, *Phys. Rev. C* **63**, 034306 (2001).
- [69] F. P. Hessberger, *Eur. Phys. J. A* **53**, 75 (2017).
- [70] P. Jachimowicz, M. Kowal, and J. Skalski, *Phys. Rev. C* **98**, 014320 (2018).
- [71] F. P. Hessberger, arXiv:2102.08793 (2021).
- [72] G. Royer, Q. Ferrier, and M. Pineau, *Nucl. Phys.* **1021**, 122427 (2022).
- [73] J. Khuyagbaatar, *Eur. Phys. J. A* **58**, 243 (2022).
- [74] S. Hofmann, F. P. Hessberger, et al., *Eur. Phys. J. A* **10**, 5 (2001).
- [75] D. Ackermann et al., *GSI Sci. Rep. 2011*, 208 (2012).
- [76] P. Ring, and P. Schuck, "The Nuclear Many-Body Problem", Springer-Verlag (New York, 1980).
- [77] N. I. Pyatov and A. S. Chernyehev, *Izv. ANSSR, seria, Fiz.* **28**, 1173 (1964).
- [78] K. Jain and A. K. Jain, *Phys. Rev. C* **3013**, (1992).
- [79] H. L. Hall et al., *Phys. Rev. C* **39**, 1866 (1989).
- [80] S. Eeckhaudt et al., *Eur. Phys. J. A* **26**, 227 (2005).
- [81] R. M. Clark et al., *Phys. Rev. Lett.* **92**, 192501 (2004).
- [82] H. B. Jeppesen et al., *Eur. Phys. J. A* **32**, 31 (2007).
- [83] A. Lopez-Martens et al., *Phys. Rev. C* **87**, 014301 (2013).
- [84] K. Hauschild et al., *Phys. Rev. Lett.* **87**, 072501 (2001).
- [85] P. T. Greenlees et al., *Phys. Rev. C* **78**, 021303(R) (2008).
- [86] D. Ackermann et al., *Nucl. Phys. A* **944**, 376 (2015).
- [87] R.-D. Herzberg et al., *Nature* **442**, 896 (2006).
- [88] A. Chatillon et al., *Phys. Rev. Lett.* **98**, 132503 (2007).
- [89] F.G. Kondev, G.D. Dracoulis, T. Kibedi, *At. Data Nucl. Data Tables* **103–104**, 50 (2015).

<https://doi.org/10.1016/j.adt.2015.01.001>

- [90] H.M. David, J. Chen, D. Seweryniak, F.G. Kondev, J.M. Gates, K.E. Gregorich, I. Ahmad, M. Albers, M. Alcorta, B.B. Back *et al.*, *Phys. Rev. Lett.* **115**, 132502 (2015). <https://doi.org/10.1103/PhysRevLett.115.132502>
- [91] J. Khuyagbaatar, A. Mistry, D. Ackermann, L.L. Andersson, M. Block, H. Brand, C. Düllmann, J. Even, F. Heßberger, J. Hoffmann *et al.*, *Nucl. Phys. A* **994**, 121662 (2020). <https://doi.org/10.1016/j.nuclphysa.2019.121662>

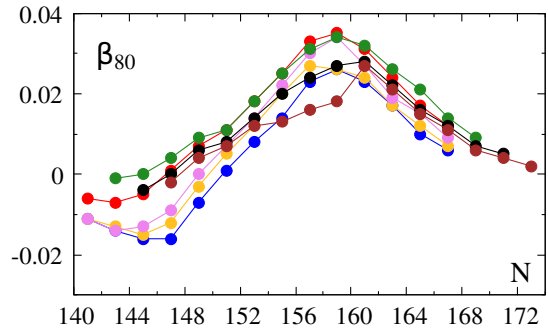
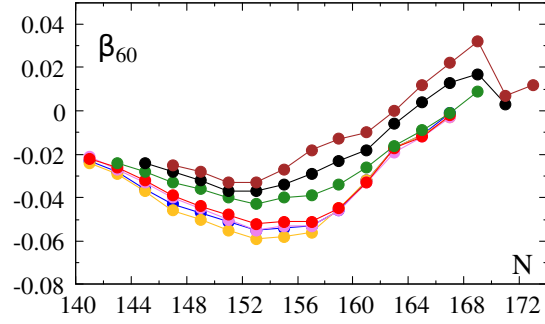
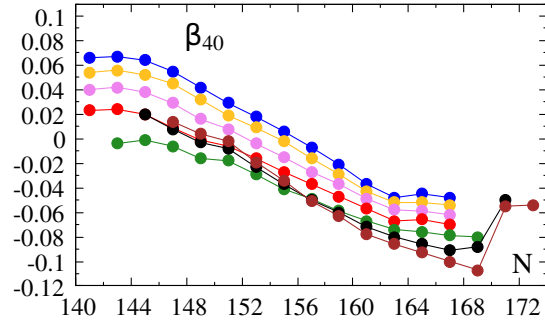
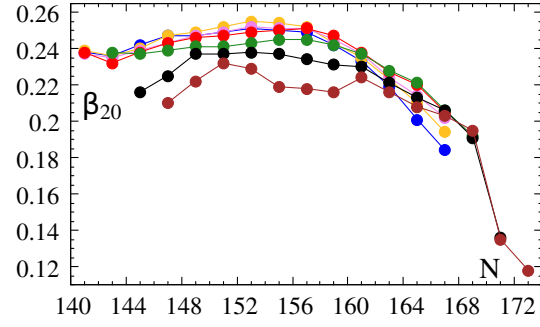


FIG. 1: Equilibrium g.s. deformations obtained in the MM model with the quasiparticle method for even-odd isotopes of: Fm - blue, No - yellow, Rf - violet, Sg - red, Hs - green, Ds - black, Cn - brown; Note different scales on the ordinate.

112				7 ⁺ 1 ⁺	9 ⁻	9 ⁻	11 ⁻	11 ⁻	3 ⁺ 1 ⁺	3 ⁺	7 ⁺	13 ⁻	3 ⁺	5 ⁺	1 ⁺ 5 ⁺	5 ⁺	15 ⁻ 1 ⁺
110			1 ⁺ 5 ⁺	7 ⁺	9 ⁻	9 ⁻	11 ⁻	11 ⁻	3 ⁺ 7 ⁺	9 ⁺	9 ⁺	13 ⁻	3 ⁺	5 ⁺	9 ⁺ 5 ⁺	5 ⁺	
108		1 ⁻ 7 ⁻	5 ⁺	7 ⁺ 9 ⁻	9 ⁻	9 ⁻	1 ⁺	1 ⁺	11 ⁻ 7 ⁺	7 ⁺ 9 ⁺	9 ⁺	13 ⁻	13 ⁻	3 ⁺	9 ⁺ 5 ⁺		
106	1 ⁻	7 ⁻ 1 ⁺	1 ⁺ 5 ⁺	7 ⁺	9 ⁻	9 ⁻	1 ⁺	1 ⁺	11 ⁻	7 ⁺	9 ⁺	13 ⁻	13 ⁻	3 ⁺			
104	1 ⁻	7 ⁻ 1 ⁺	1 ⁺	5 ⁺	9 ⁻	9 ⁻	1 ⁺	1 ⁺	11 ⁻	7 ⁺ 9 ⁺	9 ⁺	13 ⁻	13 ⁻	3 ⁺			
102	1 ⁻ 7 ⁻	7 ⁻ 1 ⁺	1 ⁺	5 ⁺	7 ⁺	9 ⁻	1 ⁺	1 ⁺	11 ⁻	7 ⁺ 9 ⁺	9 ⁺	13 ⁻	13 ⁻	3 ⁺ 9 ⁺			
100	1 ⁻ 7 ⁻	7 ⁻	1 ⁺	5 ⁺	7 ⁺	9 ⁻	1 ⁺	1 ⁺	11 ⁻	7 ⁺ 9 ⁺	9 ⁺	13 ⁻	13 ⁻	9 ⁺ 3 ⁺			
Z/N	141		145		149		153		157		161		165		169		173

FIG. 2: Ground-state spins and parities (given as $2\Omega^\pi$) of even-odd isotopes from our MM model calculated with the quasiparticle method (upper left, in black) and with the PNP (given only if different - lower right, in red).

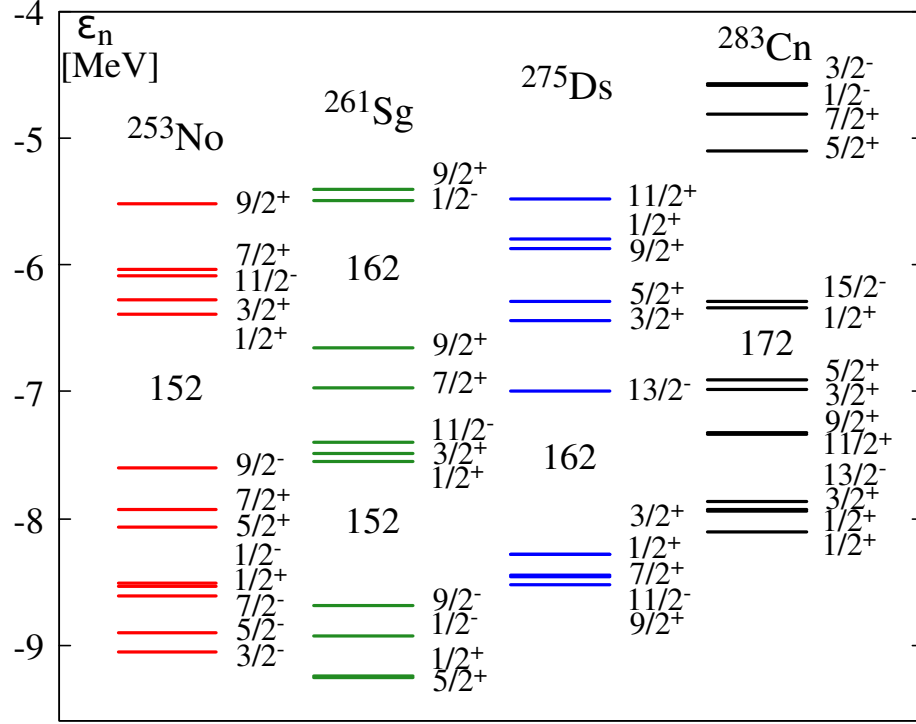


FIG. 3: Single-particle neutron levels in the Woods-Saxon potential of our MM model for four nuclei at their g.s. equilibrium deformations calculated in [59].

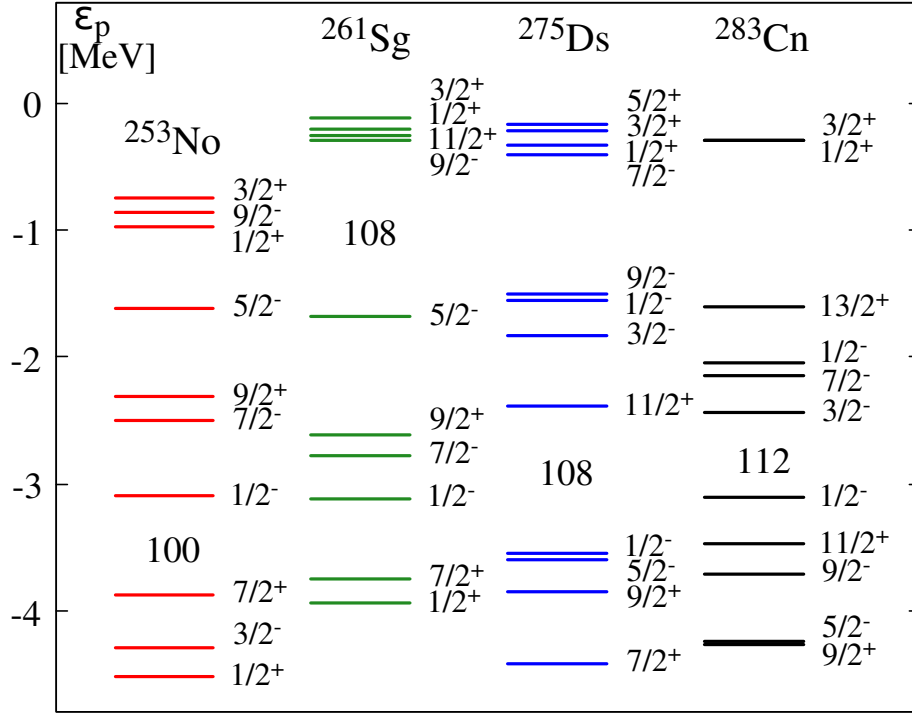


FIG. 4: Single-particle proton levels in the Woods-Saxon potential of our MM model for four nuclei at their g.s. equilibrium deformations calculated in [59].

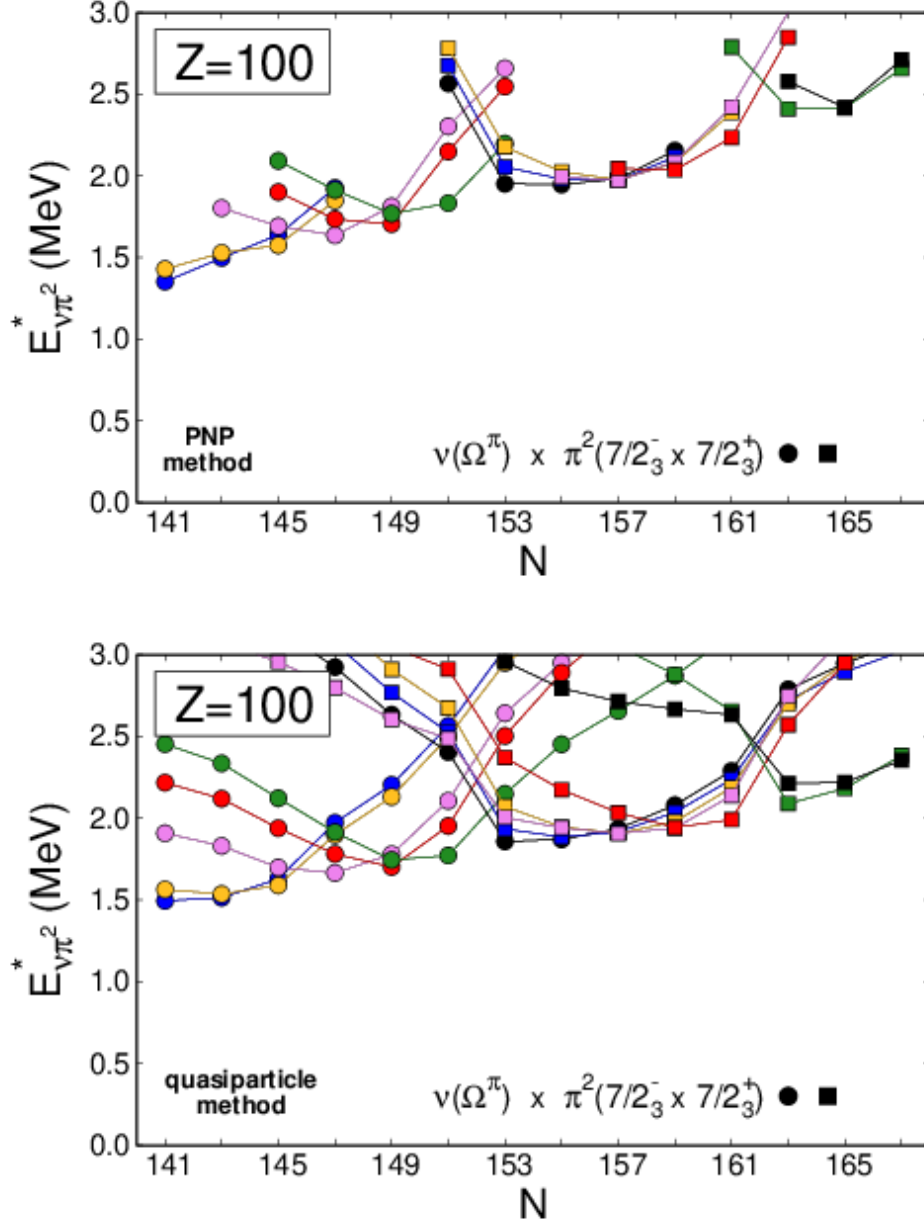


FIG. 5: Energies of low-lying $1\nu 2\pi$ large- K excitations in Fm isotopes vs N . The upper panel shows results of the PNP formalism, the lower one - of the quasiparticle method. Configurations composed of the favoured two-proton pair $\pi^2\{7/2_3^- [514] \otimes 7/2_3^+ [633]\}$ and the lowest neutron states Ω_ν^π following the rising neutron Fermi level is distinguished by the neutron component: $7/2_5^- [743]$ - blue circle, $1/2_{13}^+ [631]$ - yellow circle, $5/2_7^+ [622]$ - violet circle, $7/2_4^+ [624]$ - red circle, $9/2_3^- [734]$ - green circle, $1/2_{14}^+ [620]$ - black circle, $3/2_{10}^+ [622]$ - blue square, $11/2_2^- [725]$ - yellow square, $7/2_5^+ [613]$ - violet square, $9/2_3^+ [615]$ - red square, $13/2_1^- [716]$ - green square, $9/2_4^+ [604]$ - black square.

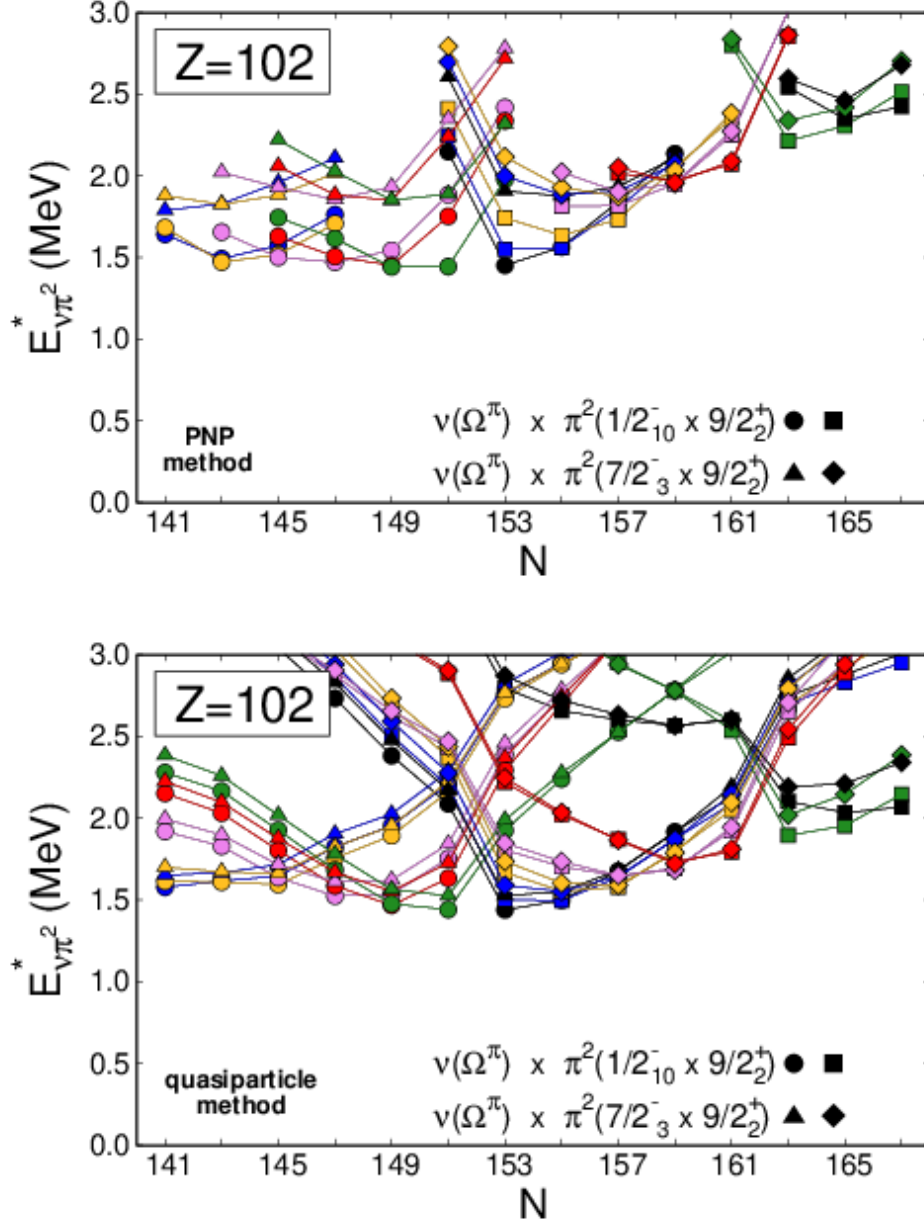


FIG. 6: As in Fig. 5 but for No isotopes. Configurations with the lowest neutron states Ω_ν^π coupled to the two-proton pair $\pi^2\{1/2_{10}^-[521] \otimes 9/2_2^+[624]\}$ are depicted by circles and squares with the colour-coding as in Fig. 5. The same neutron states coupled to the proton pair $\pi^2\{7/2_3^-[514] \otimes 9/2_2^+[624]\}$ are marked by the same colours, with circles replaced by triangles and squares by diamonds.

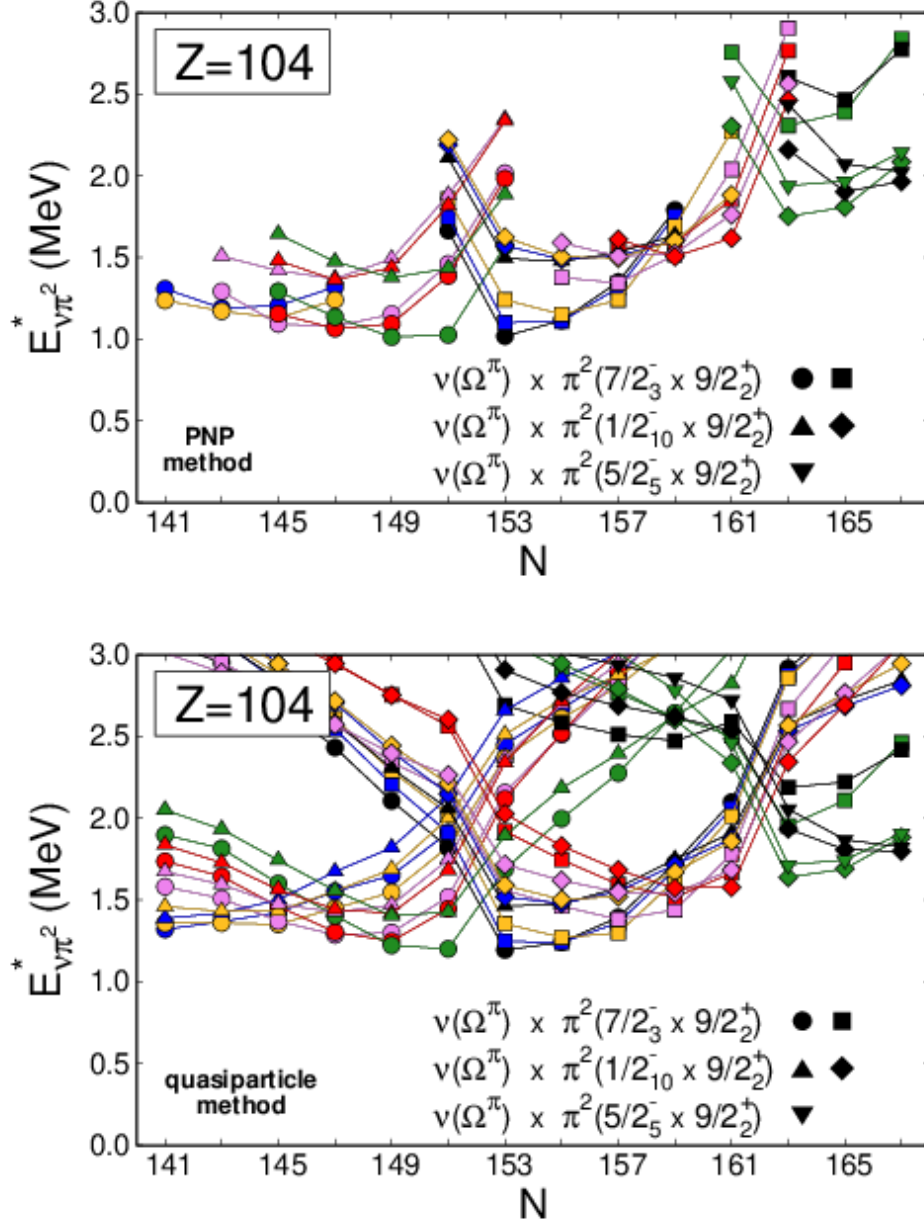


FIG. 7: As in Fig. 5 but for Rf isotopes. Configurations with two-proton pairs $\pi^2(7/2_3^- \otimes 9/2_2^+)$ and $\pi^2(1/2_{10}^- \otimes 9/2_2^+)$ are identified by their neutron components with, respectively, coloured circles/squares and triangles/diamonds as in Fig. 5. Configurations with the pair $\pi^2(5/2_5^- \otimes 9/2_2^+)$ are marked with inverted triangles, denoting the same neutron components as likely coloured squares and diamonds.

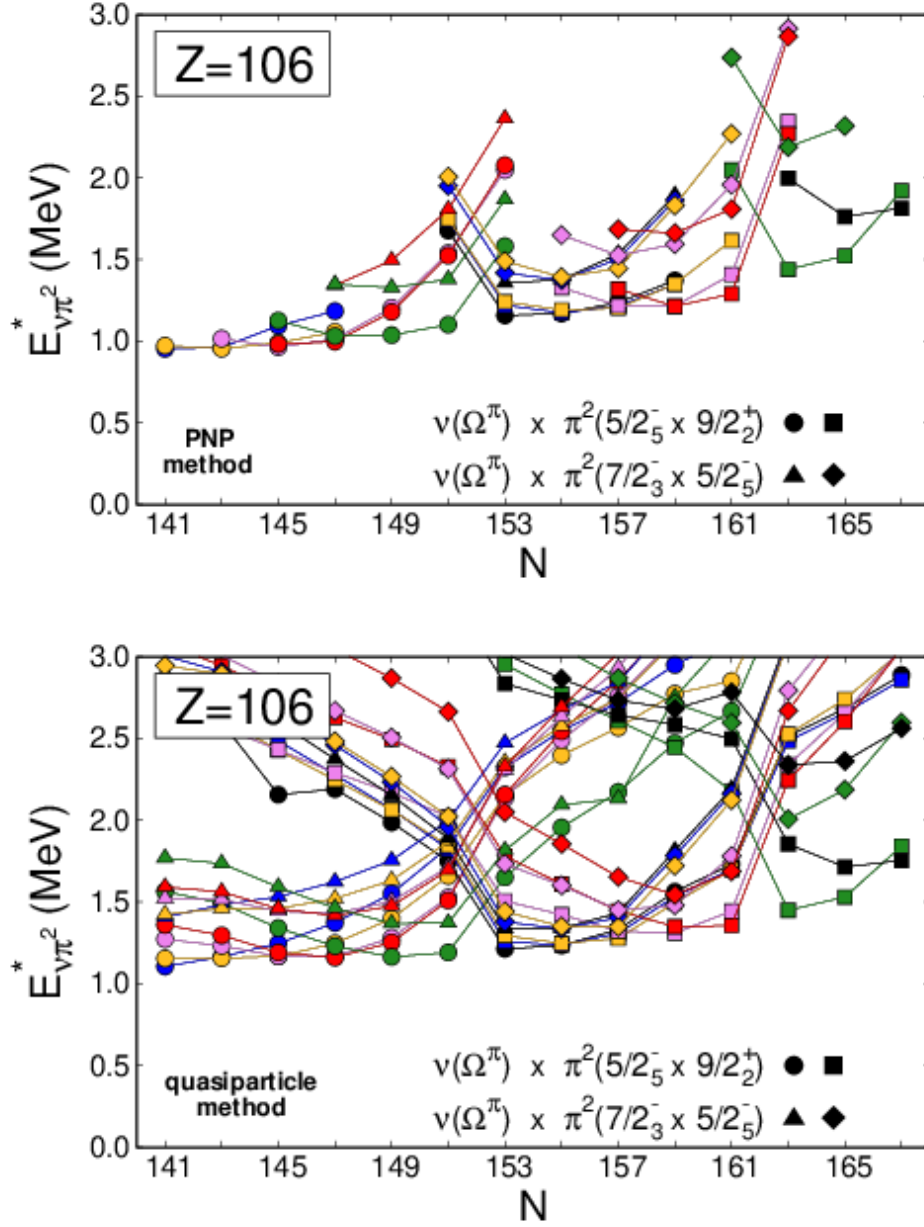


FIG. 8: As in Fig. 5 but for Sg isotopes. Coloured circles and squares refer to configurations with the $\pi^2\{5/2_5^-[512] \otimes 9/2_2^+[624]\}$ pair, triangles and diamonds - to those with the $\pi^2\{5/2_5^-[512] \otimes 7/2_3^-[514]\}$ pair, with coding analogous as in Fig. 5.

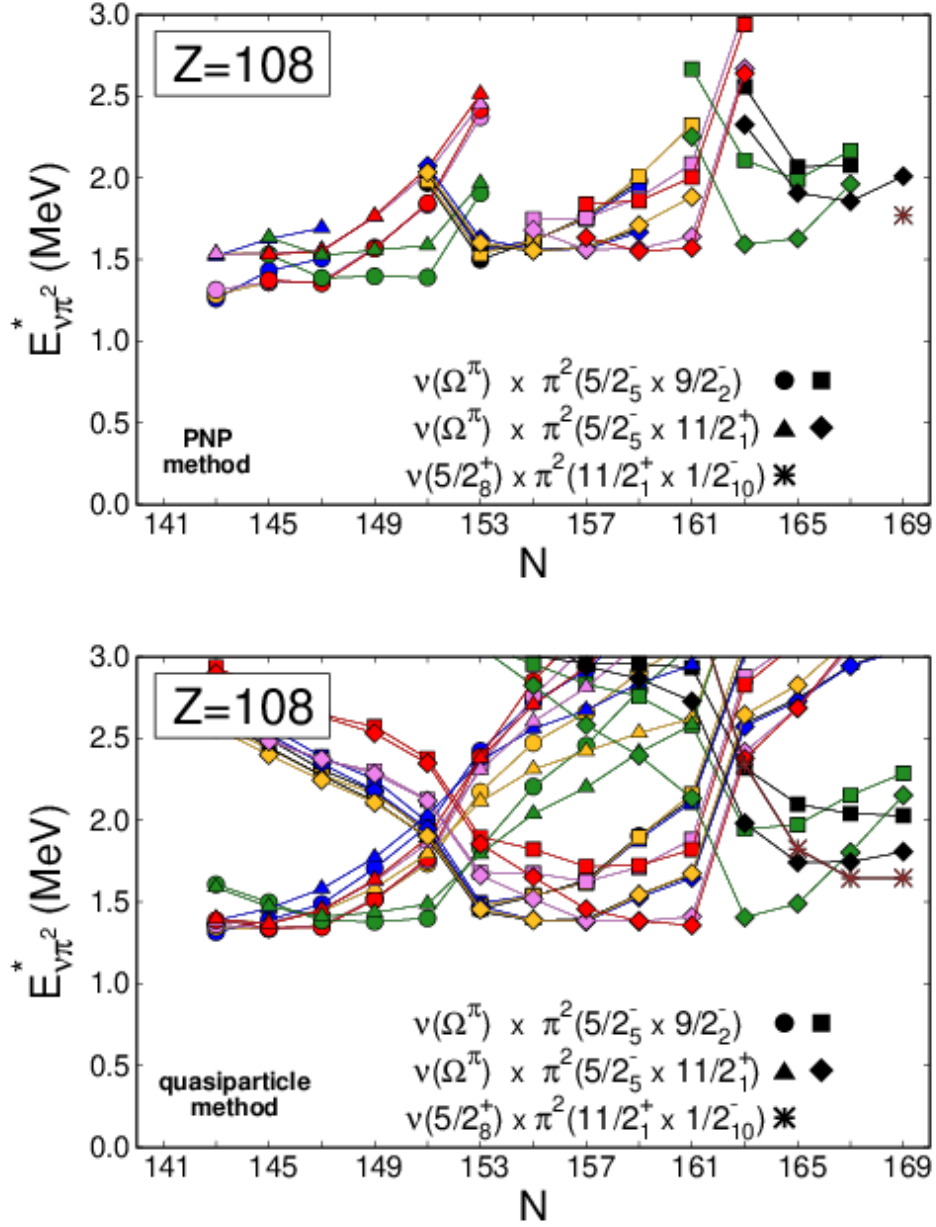


FIG. 9: As in Fig. 5 but for Hs isotopes. Configurations with the $\pi^2(5/2_5^- \otimes 9/2_2^-)$ pair (circles/squares) and $\pi^2(5/2_5^- \otimes 11/2_1^+)$ pair (triangles/diamonds) are marked in way analogous as in Fig. 8. A specific configuration $\nu 5/2_8^+ \otimes \pi^2\{11/2_1^+ \otimes 1/2_{10}^-\}$ is denoted by a brown asterisk.

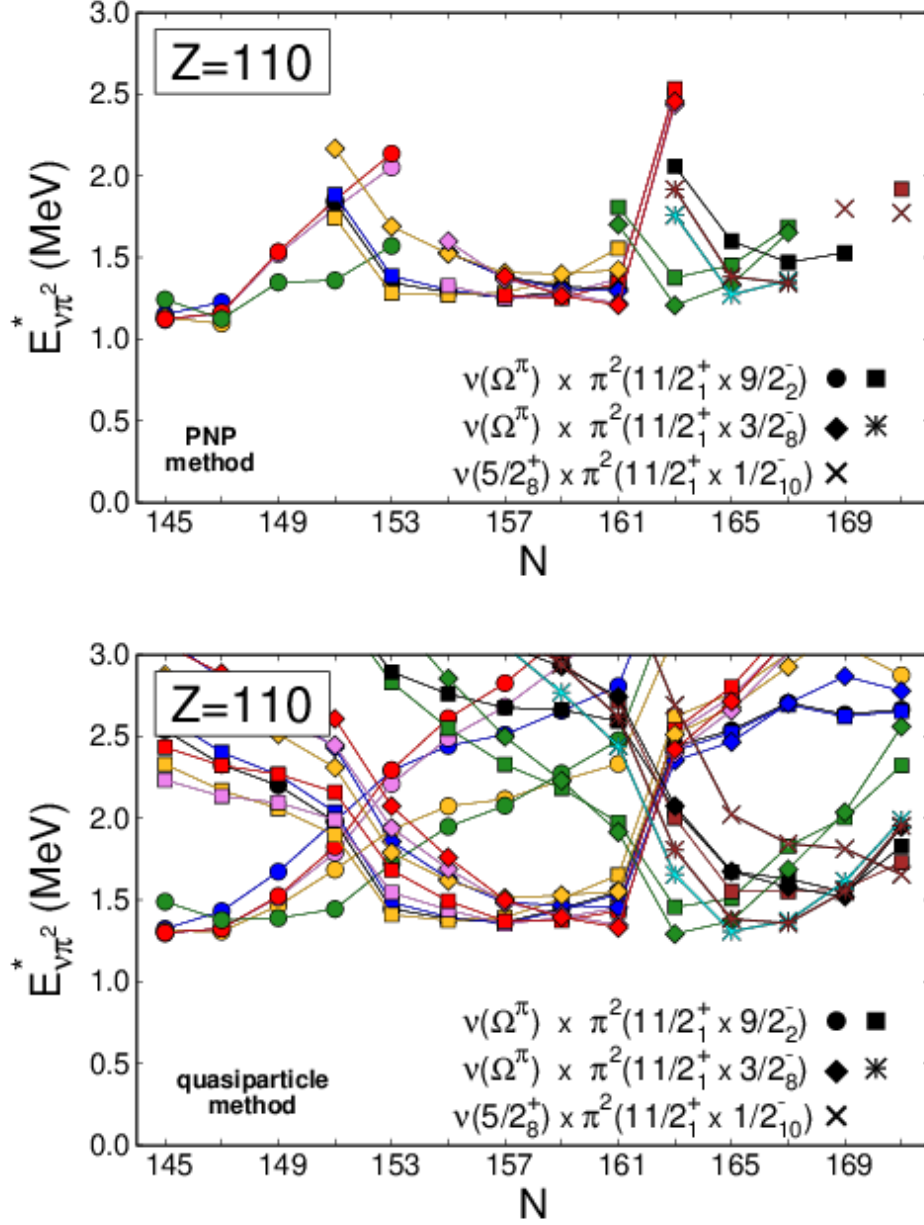


FIG. 10: As in Fig. 5 but for Ds isotopes. Configurations with the $\pi^2\{11/2_1^+[615] \otimes 9/2_2^-[505]\}$ pair are marked with coloured circles/squares as in Fig. 5; the brown square marks the same proton pair coupled to the $\nu 5/2_8^+[613]$ state. Diamonds mark the $\pi^2\{11/2_1^+ \otimes 3/2_8^-\}$ pair coupled to the same neutron components as depicted by the likely coloured squares; the same pair coupled to the $\nu 3/2_{11}^+$ and $\nu 5/2_8^+$ states are depicted by cyan and brown asterisks; the brown cross marks the $\nu 5/2_8^+ \otimes \pi^2\{11/2_1^+ \otimes 1/2_{10}^-\}$ configuration.

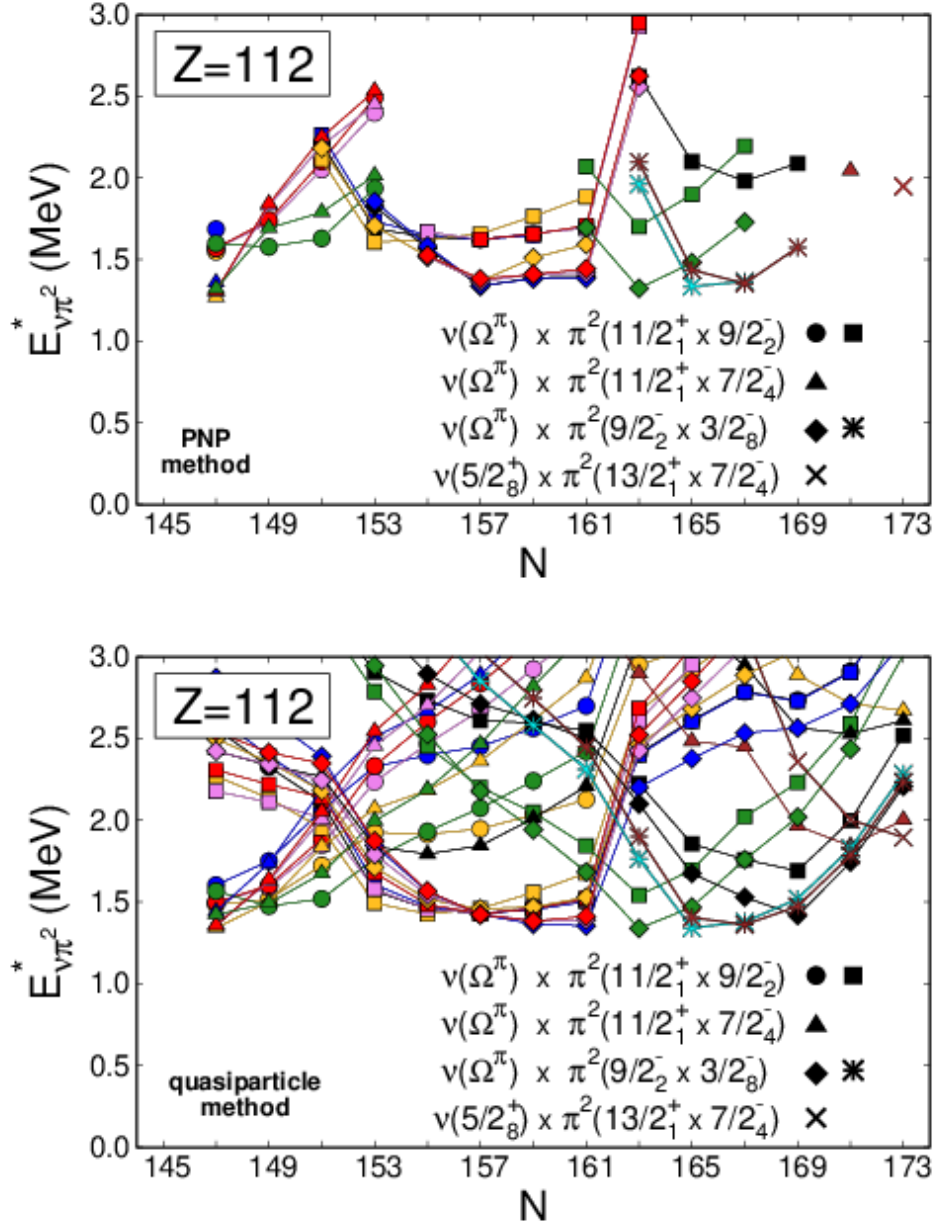


FIG. 11: As in Fig. 5 but for Cn isotopes. Configurations with the $\pi^2\{11/2_1^+[615] \otimes 9/2_2^-[505]\}$ pair are marked by circles/squares as in Fig. 10. Triangles depict the $\pi^2\{11/2_1^+ \otimes 7/2_4^-\}$ pair coupled to the same neutron states as specified by likely coloured circles, except for the brown triangle which marks the same pair coupled to the $\nu 5/2_8^+$ state. Configurations with the $\pi^2\{9/2_2^- \otimes 3/2_8^-\}$ pair marked by diamonds and asterisks have the same neutron components as likely marked configurations in Fig. 10; the brown cross marks the $\nu 5/2_8^+ \otimes \pi^2\{13/2_1^+ \otimes 7/2_4^-\}$ configuration.

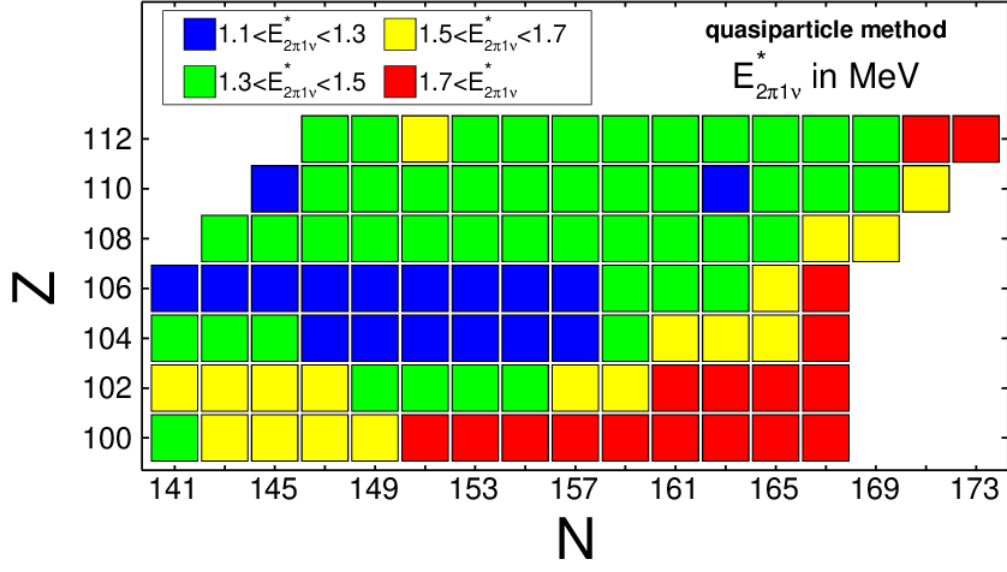


FIG. 12: Map of the lowest $1\nu 2\pi$ 3-q.p. excitation energies calculated with the quasiparticle method.

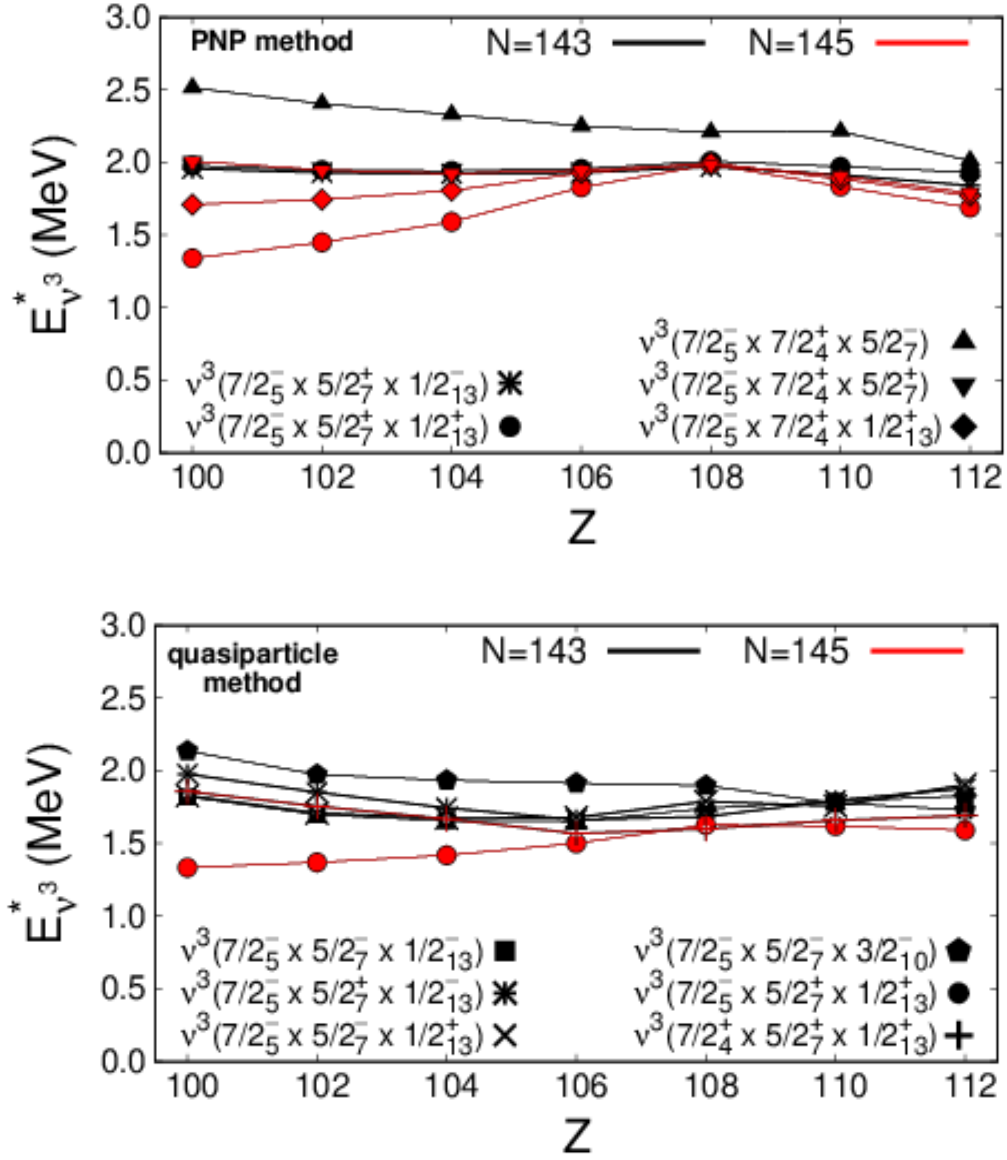


FIG. 13: Excitation energies of low-lying high- K 3ν configurations in $N = 143, 145$ isotones. Colours distinguish N , point shapes mark configurations.

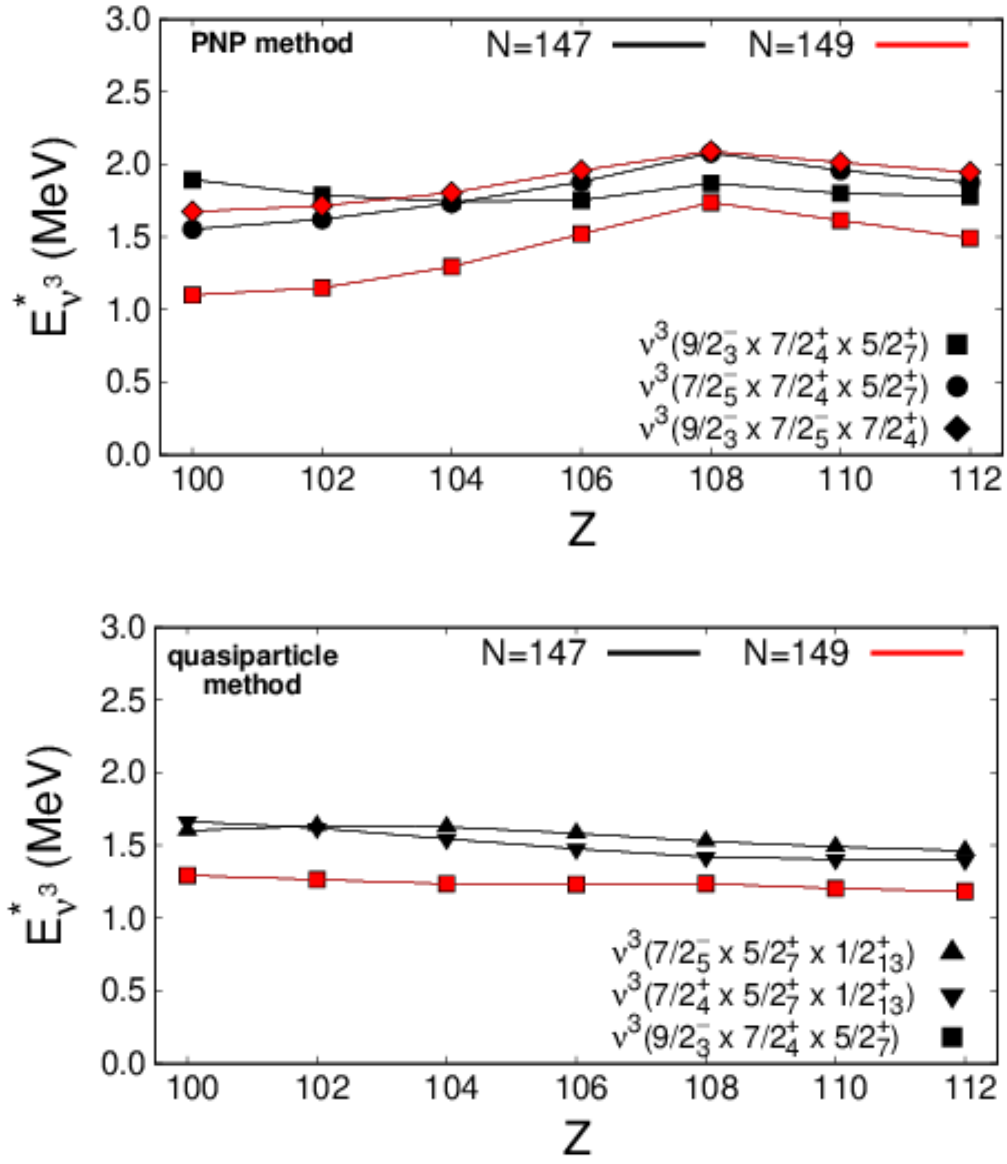


FIG. 14: As in Fig. 13, but for $N = 147, 149$ isotones.

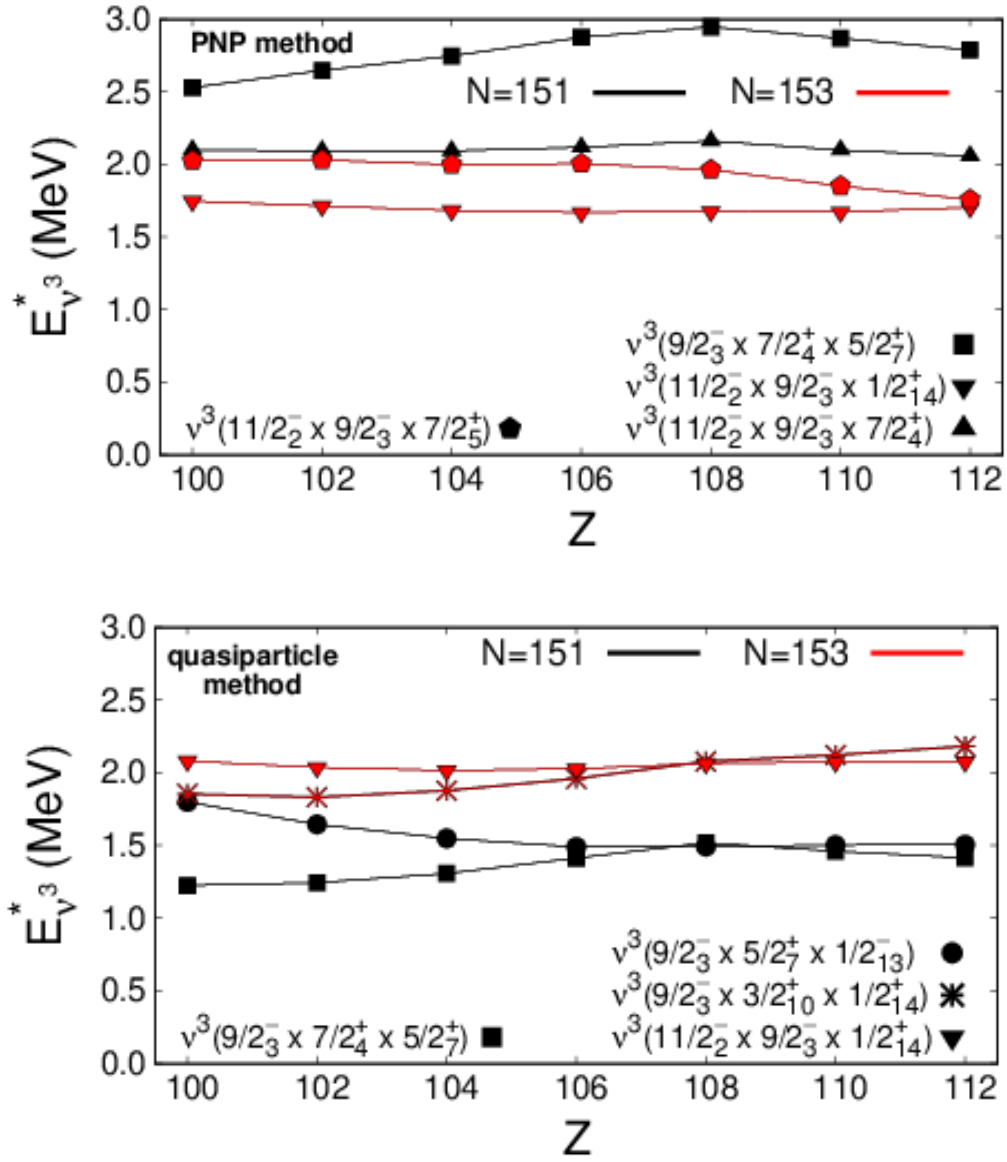


FIG. 15: As in Fig. 13, but for $N = 151, 153$ isotones.

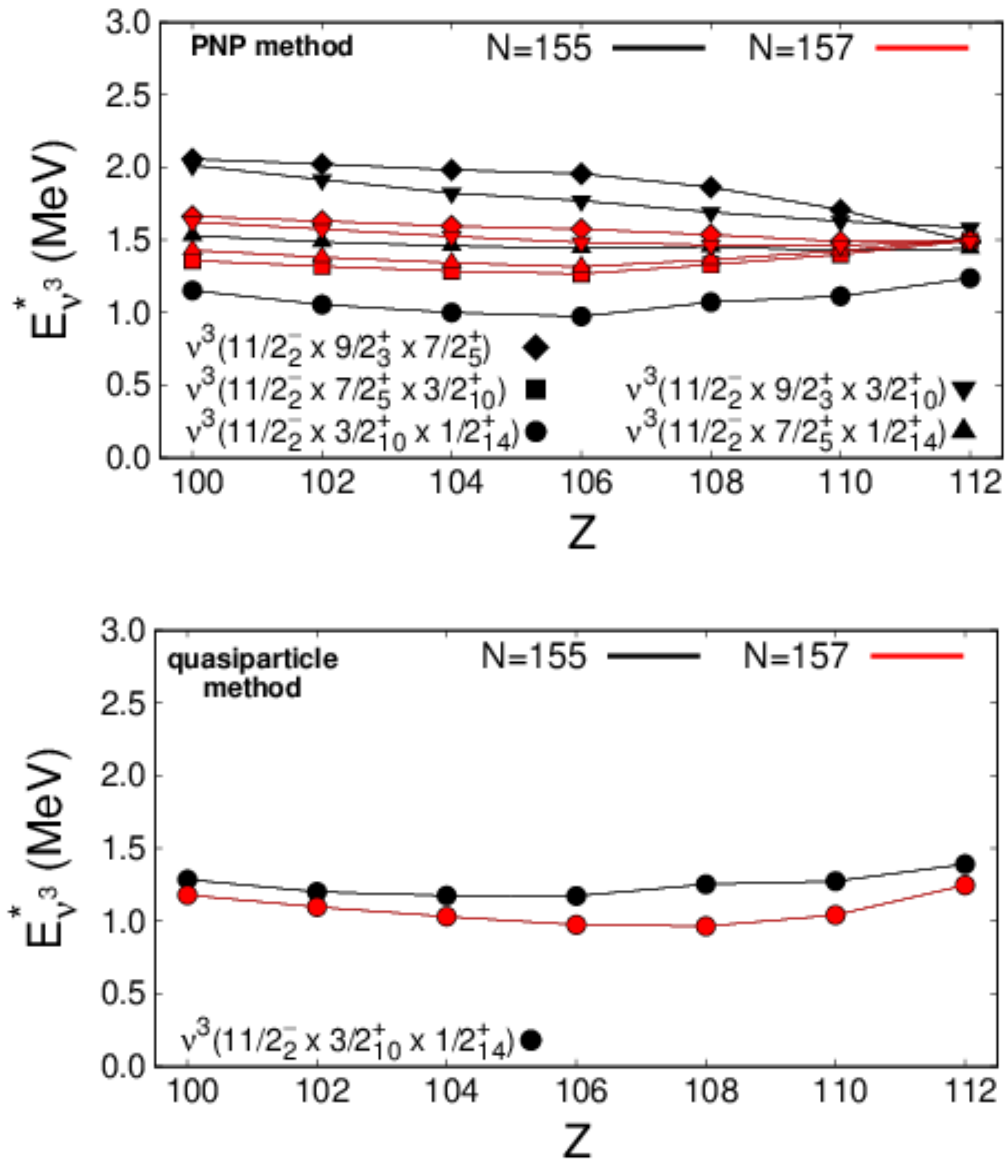


FIG. 16: As in Fig. 13, but for $N = 155, 157$ isotones.

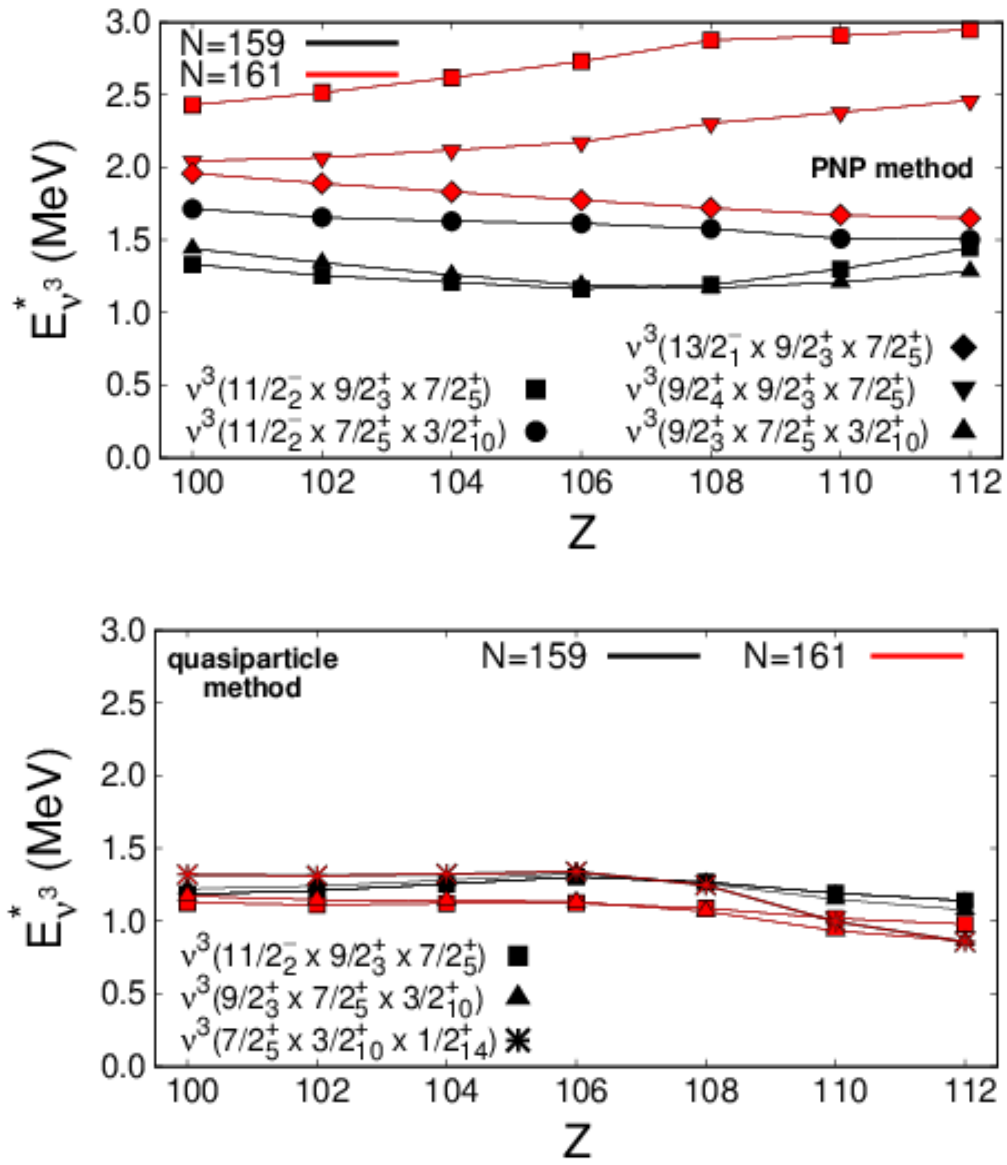


FIG. 17: As in Fig. 13, but for $N = 159, 161$ isotones.

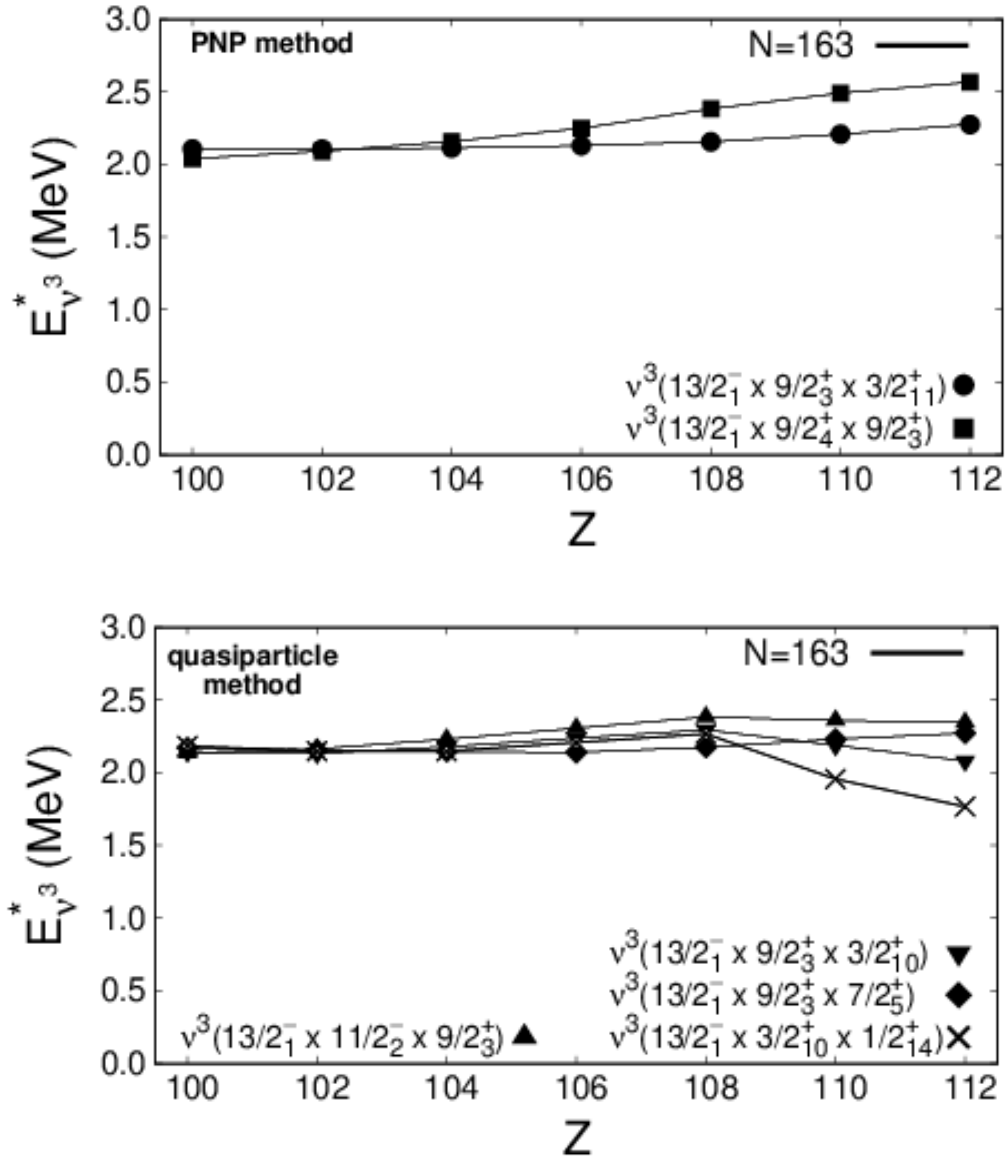


FIG. 18: As in Fig. 13, but for $N = 163$ isotones.

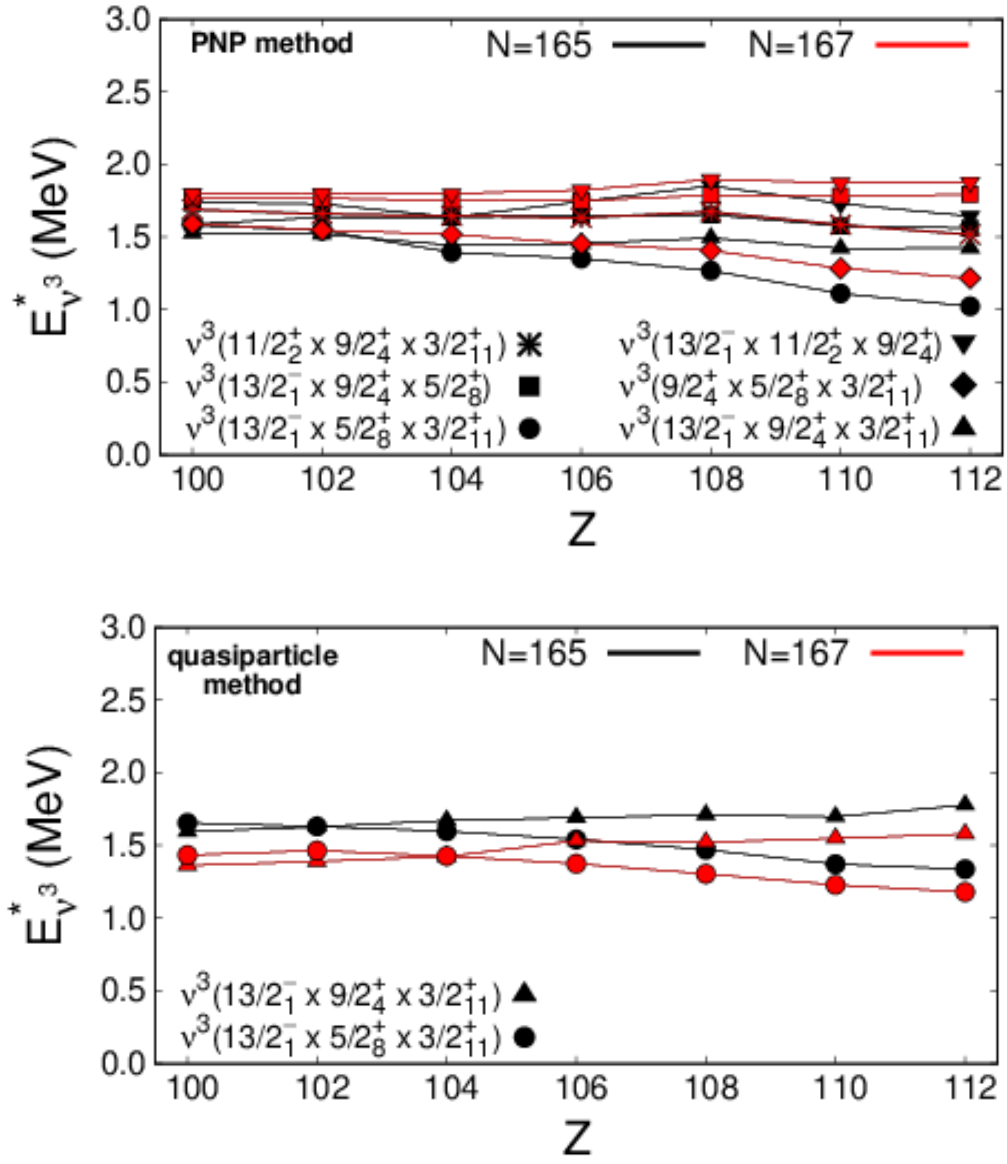


FIG. 19: As in Fig. 13, but for $N = 165, 167$ isotones.